



UNIVERSITEIT•STELLENBOSCH•UNIVERSITY  
jou kennisvennoot • your knowledge partner

# Design of a haptic controller for excavators

by

Lodewyk Francois van der Zee



*Thesis presented at the University of  
Stellenbosch in partial fulfilment of the  
requirements for the degree of*

Masters of Science in Engineering

Department of Electrical Engineering  
University of Stellenbosch  
Private Bag X1, 7602 Matieland, South Africa

Supervisors: Dr. M. Blanckenberg  
Mr. N.F. Treurnicht

March 2009

# Declaration

I, the undersigned, hereby declare that the work contained in this thesis is my own original work and that I have not previously in its entirety or in part submitted it at any university for a degree.

Signature: .....

L. F. van der Zee

Date: .....

Copyright © 2009 University of Stellenbosch  
All rights reserved.

# Abstract

The input orientation of the excavators in use today usually comprises two joysticks that control the actuator links individually. In order to perform an excavation task, several different combinations of joystick inputs are required, placing high psychomotor demands on the operator. In training an operator this creates a steep learning curve, with a lengthy training time and a reasonable amount of experience being required to perform an excavation task skilfully. In this master's thesis a haptic<sup>1</sup> device was developed, resolving input ergonomics and creating a single input device capable of providing feedback to the operator. The design and construction of the haptic device, with the related control scheme, is presented and discussed. The control scheme combines position and rate control, and relates all the actuator joint positions to a single end-effector point. The control and ergonomic aspects of the haptic device were tested and compared to the traditional two joystick control setup by means of the implementation of a virtual excavator simulator. The simulation was developed in MATLAB, and virtual excavator displayed in an OpenGL window. The objective of this study was to evaluate the human factors related to the input orientation. Ten inexperienced test subjects were recruited to perform four sets of tests, where each test required a different level of operator skill. The results indicated that, on average, the test subjects had an increased level of performance after training on the haptic device. These results strongly support the hypothesis that haptic control simplifies the operational tasks required for operating an excavator.

---

<sup>1</sup>The word haptic means of, or relating to, the sense of touch, or tactile

# Opsomming

In die algemeen bestaan die inset oriëntasie van sloopgrawers uit twee beheerstokke wat elke hidrouliese aktueerder apart beheer. As die operateur 'n graaf aksie wil uitoefen vereis dit dat hy die twee beheerstokke gelyktydig met verskillende aksies moet beheer. Die gelyktydige beheer van die beheerstokke plaas baie druk op die operateur se hand-en-oog koördinasie vermoë, wat 'n strawwe leerkurwe veroorsaak en 'n lang opleidingstydperk tot gevolg het. In die projek is 'n haptiese beheerstok ontwikkel wat die ergonomika-probleem aanspreek en die moontlikheid bied om terugvoer te gee. Die ontwerp en konstruksie van die haptiese beheerstok, sowel as die beheermetode, word beskryf en bespreek in die tesis. Die beheermetode is 'n kombinasie van posisie- en tempobeheer waar al die aktueerder arms beheer word na 'n enkele posisie eindpunt of bak posisie. Die beheer en ergonomiese aspekte van die haptiese beheerstok was vergelyk met die oorspronklike twee-beheerstok oriëntasie deur middel van 'n virtuele sloopgrawer simuleerder. Die simuleerder is in MATLAB ontwikkel, en vertoon in 'n OpenGL venster. Die doel van die toetse was om menslike faktore verwant aan die inset uitleg te vergelyk. Tien onopgeleide gewilliges is gevra om vier stelle toetse af te lê, waar elke toets 'n ander hoeveelheid operatorsvaardigheid verg. Die resultate het aangedui dat die gemiddelde werkverrigting van die operateurs beter was met die haptiese beheerstok as met die twee-beheerstok opstelling. Die resultate ondersteun die stelling dat haptiese beheer die beheertake van 'n sloopgrawer operateur vereenvoudig.

# Acknowledgements

I would like to express sincere gratitude to the following people who have contributed to making the project work:

- Dr M. Blanckenberg, for the huge amount of technical help, guidance, support and funding of the project
- Mr N. Treurnicht for the help on the initial design concepts and ergonomic problems
- Mr W. Croukamp for the construction and insights on the mechanical design
- Ms A.J. van der Spuy for her editorial support

And last, but certainly not least, I exalt God for the wisdom and perseverance that He has bestowed on me during this project, and throughout my life.

# Dedications

*My parents and Leanne for their love, inspiration and support*

# Contents

<b>Declaration</b>	<b>i</b>
<b>Abstract</b>	<b>ii</b>
<b>Opsomming</b>	<b>iii</b>
<b>Acknowledgements</b>	<b>iv</b>
<b>Dedications</b>	<b>v</b>
<b>Contents</b>	<b>vi</b>
<b>List of Figures</b>	<b>ix</b>
<b>List of Tables</b>	<b>xi</b>
<b>Nomenclature</b>	<b>xii</b>
<b>1 Introduction</b>	<b>1</b>
<b>2 Literature review</b>	<b>5</b>
<b>3 Modelling</b>	<b>10</b>
3.1 Labelling convention and notation . . . . .	10
3.2 Forward Kinematics . . . . .	12
3.3 Inverse kinematics . . . . .	15
3.4 Summary . . . . .	17

<b>4</b>	<b>Design and construction</b>	<b>18</b>
4.1	Concept design . . . . .	18
4.2	Detailed mechanical design . . . . .	23
4.2.1	Rotation actuator . . . . .	23
4.2.2	Linear actuator . . . . .	24
4.2.3	Wrist and bucket action . . . . .	26
4.3	Motor controller design . . . . .	27
4.3.1	MOSFET driver . . . . .	29
4.3.2	Strain gauge amplifiers . . . . .	30
4.3.3	Opto-couplers . . . . .	30
4.3.4	dsPIC controller . . . . .	31
4.4	Summary and final design . . . . .	31
<b>5</b>	<b>Virtual excavator and simulator software</b>	<b>34</b>
5.1	Graphical interface . . . . .	35
5.1.1	GLwidget . . . . .	35
5.1.2	Window . . . . .	38
5.1.3	Network server . . . . .	38
5.1.4	File loader . . . . .	39
5.2	MATLAB simulation . . . . .	39
5.2.1	Input functions . . . . .	40
5.2.2	Input control and kinematics . . . . .	40
5.2.3	MATLAB client . . . . .	41
5.2.4	Evaluation block sets . . . . .	41
<b>6</b>	<b>Test procedures and results</b>	<b>47</b>
6.1	Test 1: Orientation . . . . .	48
6.1.1	Comments on test 1 . . . . .	50
6.2	Test 2: Following desired trajectory . . . . .	51
6.2.1	Comments on test 2 . . . . .	53
6.3	Test 3: Grading . . . . .	54
6.3.1	Comments on test 3 . . . . .	58
6.4	Test 4: Excavation . . . . .	58

<i>CONTENTS</i>	<b>viii</b>
6.4.1 Comments on test 4 . . . . .	59
6.5 Summary and discussion . . . . .	61
<b>7 Summary and recommendations</b>	<b>64</b>
7.1 Summary . . . . .	64
7.2 Recommendations . . . . .	65
7.2.1 General . . . . .	65
7.2.2 Mechanical . . . . .	65
7.2.3 Control . . . . .	66
7.2.4 Simulator . . . . .	66
<b>Appendices</b>	<b>68</b>
<b>A Statistical summary</b>	<b>69</b>
<b>B Design dimensions</b>	<b>70</b>
<b>C Hardware details</b>	<b>72</b>
<b>Bibliography</b>	<b>75</b>

# List of Figures

1.1	Illustration of conventional two lever setup . . . . .	2
1.2	Illustration of conventional four lever setup . . . . .	3
3.1	Positive sense for $\alpha_i$ and $\theta_i$ . . . . .	12
3.2	Excavator joint angles and component frames . . . . .	13
3.3	Illustration of the bucket angle . . . . .	15
3.4	Excavator joint angles and component frames for inverse kinematics . . . . .	16
4.1	Concept design of haptic device . . . . .	20
4.2	Illustration of control scheme . . . . .	21
4.3	Illustration of control scheme and regions . . . . .	22
4.4	Rotation actuator . . . . .	24
4.5	Linear actuator . . . . .	25
4.6	Wrist and trigger . . . . .	27
4.7	Conceptual overview of motor controller . . . . .	28
4.8	Application diagram of the H-bridge . . . . .	29
4.9	Simplified circuit diagram of strain gauge amplifier . . . . .	30
4.10	Calculation steps taken with motor control . . . . .	32
4.11	Illustration of the constructed haptic device - actual haptic on the left and the CAD model on the right . . . . .	33
5.1	Interaction of software modules . . . . .	34
5.2	Block sets and functions . . . . .	36
5.3	Block diagram of the GLwidget class . . . . .	37

5.4	Graphical interface with a side view of the excavator links . . .	38
5.5	MATLAB simulink model with excavation block . . . . .	39
5.6	Calculation steps of Orientation block . . . . .	42
5.7	Calculation steps of Trace block . . . . .	43
5.8	Calculation steps of Grade block . . . . .	45
5.9	Calculation steps of Excavation block . . . . .	46
6.1	Screenshot of test 1 - Orientation . . . . .	49
6.2	Test 1 completed with joystick . . . . .	50
6.3	Distance vs. time: Test 1 - Orientation . . . . .	50
6.4	User results of test 1 - Orientation . . . . .	51
6.5	Screenshot of test 2 - Following desired trajectory . . . . .	52
6.6	Test 2 completed with joystick . . . . .	52
6.7	Distance vs. time: Test 2 -Following desired trajectory . . . . .	53
6.8	User results of test 2 - Following desired trajectory . . . . .	54
6.9	Screenshot of test 3 - Grading . . . . .	55
6.10	Test 3 completed with joystick . . . . .	56
6.11	Test 3 completed with haptic device . . . . .	56
6.12	User results of test 3 - Grading . . . . .	57
6.13	Screenshot of test 4 - Excavation . . . . .	59
6.14	Test 4 completed with joystick . . . . .	60
6.15	Distance vs. time: Test 4 - Excavation . . . . .	60
6.16	User results of test 4 - Excavation . . . . .	61
B.1	General dimensions of haptic device . . . . .	71

# List of Tables

3.1	Denavit-Hartenberg parameters . . . . .	13
4.1	Workspace and control regions of actuators . . . . .	22
4.2	DC motor characteristics of the rotation actuator . . . . .	24
4.3	DC motor characteristics of the linear actuator . . . . .	26
4.4	Strain gauge comparison and output relative to force input . .	31
6.1	Summary of the average improvement for the four tests . . . .	62
6.2	Summary of the three main improved areas . . . . .	62
C.1	H-bridge PC board details . . . . .	72
C.2	dsPIC PC board details . . . . .	73
C.3	Opto-coupler PC-board details . . . . .	73
C.4	Stain gauge PC-board details . . . . .	73
C.5	Load cell PC-board details . . . . .	74
C.6	Truth table for the HIP4081; X signifies that input can be either a 1 or 0 . . . . .	74

# Nomenclature

## Greek Letters

$\alpha$	Twist angle
$\theta$	Joint angle
$\phi$	Bucket angle with ground plane $X_0$ - $Y_0$

## Capital Letters

$F$	Force
$M_s$	Motor speed
$V_l$	Actuator speed
$T_R$	Torque required

## Small Letters

$a$	Link length
$d$	Joint offset
$d_m$	Screw diameter
$f$	Friction coefficient
$l$	screw pitch
$r$	Distance between link origins

## Acronyms

2D	Two Dimensional
3D	Three Dimensional

ADC	Analog to Digital Converter
AVG	Average
DC	Direct Current
DH	Denavit-Hartenberg
dsPIC	Digital Signal Programmable Interrupt Controller
MOSFET	Metal Oxide Semiconductor Field Effect Transistor
POT	Potentiometer
PWM	Pulse With Modulation
RPM	Revolutions per minute
SD	Standard deviation
UART	Universal Asynchronous Receiver/Transmitter
UDP	User Datagram Protocol
USB	Universal Serial Bus

**Units**

A	Ampere
g	Gram
Hz	Hertz
m	Metres
N	Newton
V	Volt
s	Seconds
$\Omega$	Ohm

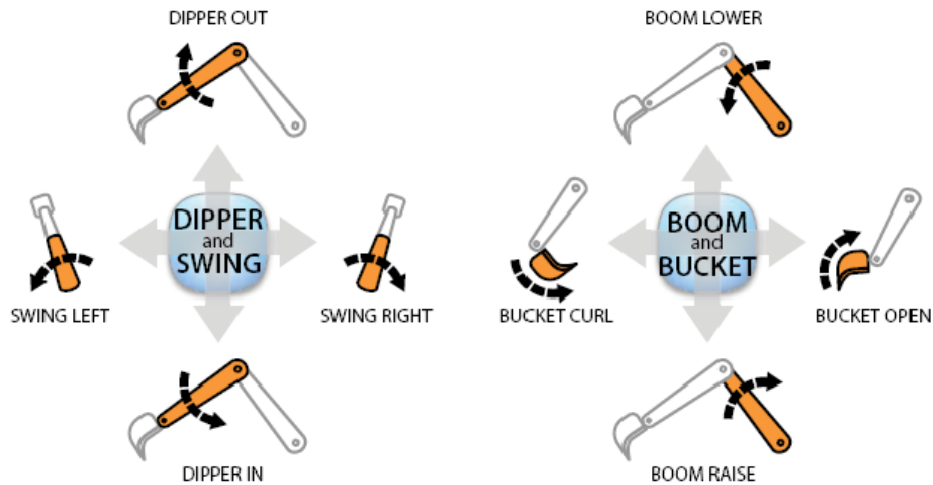
# Chapter 1

## Introduction

In a country such as South Africa, where construction has great economic significance, a shortfall of both skilled labour and technological advances in construction raises concern. The problem addressed in this Master's project is the design and implementation of an excavator control system. The controller design focuses on the simplification of difficult excavation tasks and the implementation of an ergonomic user interface; making it easier to acquire the skills needed by an operator. Several tasks concerned with earthmoving, such as trenching and footing formation, require precisely executed control movements.

In conventional earthworking implements, such as excavators, the bucket and arms are moved by the extension and retraction of hydraulic cylinders. The traditional way of controlling the hydraulic cylinders is by the use of manually controlled proportional valves. A gear pump produces oil flow which is constant at any engine speed of the excavator. At idle the oil flows continuously at a constant pressure until it is directed to a load or cylinder via a proportional valve. This causes a rise in pressure which is greater than the resistance, resulting in cylinder displacement. The operator controls the flow by displacing the spools in the valves; the extent of the spool displacement being directly related to the velocity at which the cylinder extends or retracts. The spool displacement is controlled by the operator through a direct mechanical connection or lever.

Generally the function of the excavator actuator is replaced by either a single axis control lever, or a dual joystick which combines two functions of movement.



ISO, SAE and 'EXCAVATOR' PATTERN

Figure 1.1: Illustration of conventional two lever setup

In a conventional backhoe, four actuator functions are controlled, including boom swing, boom elevation, crowd or elbow angle, and bucket curl or pitch. Thus a minimum of two dual axis levers or, more conventionally, four single axis levers are required to control the bucket of an excavator. The two or four control levers do not resemble the configuration of the bucket arm, so that learning to control a excavator by its levers is not intuitive. An operator must learn to associate the labelled name of a lever, or its position in relation to the other levers, with the backhoe function it controls. The control actions related to each cylinder of the four lever and the dual joystick configurations are illustrated in figures 1.1 and 1.2. When the operator is required to dig a trench a combination of control actions must be performed simultaneously to keep the bucket

level at the desired depth. The boom and dipper must be raised and lowered in relation to the bucket's height while maintaining the correct bucket angle. Thus the operator must perform the inverse kinematics in his head in order to perform the desired action or trajectory correctly.

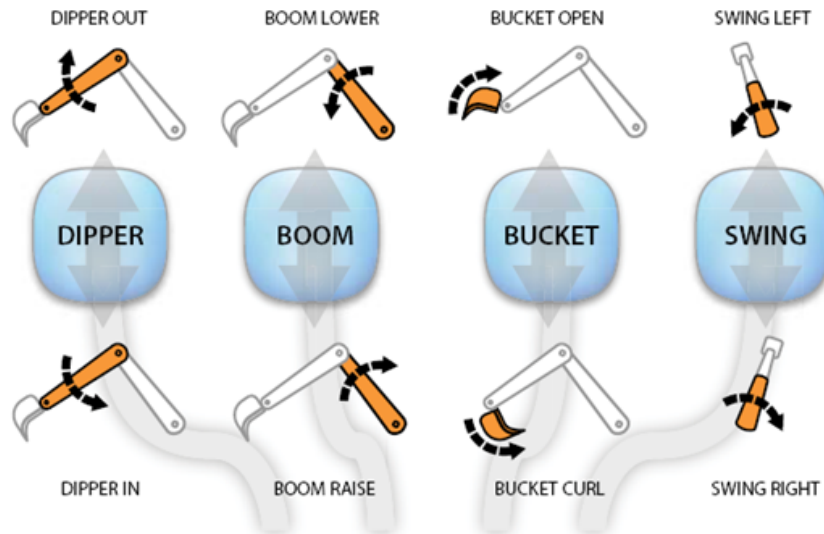


Figure 1.2: Illustration of conventional four lever setup

An additional problem, particularly with four levers, is that the efficiency of operation of the backhoe suffers as a result of the operator having to switch hands from lever to lever to coordinate the movements of the bucket. The operator also finds it extremely difficult to relate the forces exerted on the end-effector to the control functions he is performing, since the only feedback that he receives is the observed movement and orientation of the end-effector. As a result of these and other factors, considerable expense and practice time is required to train a proficient and safe backhoe operator [1].

The solution, and the intention of the project, is to create an ergonomic single input device that relates all the joint positions to a single end-effector point. The implementation is expected to greatly reduce the training time, as the operator thinks and works solely in Cartesian space.

The forces experienced by the end effector could be translated and displayed through a haptic device<sup>1</sup>. Control signals for each valve can be derived by simplifying several of the excavation tasks and allowing automated control as well as by the implementation of tele-operated control.

The main focus of the project was the ergonomic design of the input device. There have been several implementations of haptic control with hydraulic equipment, where the haptic device used was an "off the shelf" input device lacking robustness and the desired ergonomic aspects. A haptic input device was designed and built in conjunction with a virtual excavator environment. The control achieved is illustrated by simulating the movements and excavation tasks in MATLAB via a virtual interface in OpenGL. The orientation of the input device was designed to obtain the most ergonomic and work efficient orientation. Several input orientations (position and rate) are incorporated. The control system implemented relates the Cartesian space inputs to the joint angles and kinematic orientation. The human factors related to the two different control orientations were also compared and evaluated after rigorous testing via the simulator.

The material presented will describe the initial work done to simulate the interaction of the haptic with the backhoe. Information presented in this thesis is divided into two main categories: 1) modelling and design 2) construction and validation with initial testing. In the first category a mathematical model will be derived for the backhoe dynamics and kinematics transformations and simulated for verification of control algorithms. In the second category, the mechanical design and software for the haptic input device will be presented. The simulation software used will also be discussed as will the simulated interactive environment. The training time on a virtual simulator and input layout will be documented and discussed. Finally, suggested areas of future research on the current system will be proposed.

---

<sup>1</sup>The word haptic means of or relating to the sense of touch, or tactile

# Chapter 2

## Literature review

The first part of the literature study was undertaken in order to obtain information on the classic input control of excavators and backhoes. The control actions which are necessary for the operator to perform traditional excavation task such as trenching and digging are described by Coughlin [2], where several operational tasks and instructions are given in order to produce a smooth, efficient execution. The training time and experience required to produce a professional backhoe operator was also studied and noted by Bernold [1]. A comparison of the types of input control preferred by the operator is given by Luengo et al [3]. Research has also been done to optimise the digging process by automating different aspects of the excavator process [4], [5]. A fully automated excavator has been implemented and this is illustrated in Stentz et al [6].

The latest field of electro-hydraulic control, which is expanding significantly, is the haptic control of hydraulic equipment. The ability to measure the force exerted, by reflection, as well as to exert coordinated control; enhances the operation of machinery by humans. The only way to measure the performance enhancement is through the testing of human factors [7], [8]. The human factor testing most relevant to this project was conducted on ten novice and six experienced log loader operators [7]. The operators performed loader tasks with both control orientations; the results were then noted and compared. Interestingly enough, it was

found that initially the novice operators had experienced an increase in their levels of performance, while the experienced operators had a decreased level of performance on the coordinated control. After five days of testing the experienced operator's performances on the two different control orientations converged. This indicated an improved learning curve, demonstrating the same proficiency as they had shown with the uncoordinated control that they were accustomed to.

A great deal of research has been conducted on haptic devices, the two main areas being 1) the interaction of haptic devices between virtual environments and 2) the implementation of haptic devices in teleoperated tasks. Virtual simulation uses the haptic device to create a certain feeling or increased awareness (eg flight simulators), whereas the teleoperated haptic system uses the haptic device more to relate forces that are felt by the mechanism or robot (i.e. a robot arm servicing a nuclear steam generator). Other applications that relate to a combination of the two main research fields are tactical aids for the visually impaired [9] and assistance with manufacturing and assembly [10].

The design goal of the haptic controller is to produce a haptic device that is both stable and transparent, where the user cannot distinguish between operating the excavator and operating the haptic device [11]. The main design concern is the relationship between the haptic work space and the excavator work space. Several literature studies are available that document the combination of a number of control strategies; position control, rate control, force control and impedance control. Position control is the simplest to implement, where the position of the haptic device, or master, relates directly to the position of the slave or backhoe. Position control delivers satisfactory results during unconstrained motion, but unfortunately problems arise when external forces are present (eg the interaction between the end-effector and the soil) [12]. Alternatively a system may be implemented where the user can switch between control modes when the end-effector comes into contact with the soil. The second and most widely used method of control is rate control, where a velocity command is generated with relation to the position of the master

or joystick. Rate control is also preferred by most operators, as it results in better performance and accuracy [3]. The third method is force control, where the force produced by the excavator's actuators is related to the master-joystick position. Examples of force control are documented in [13] where a reference is tracked in such a way that the desired force is exerted on the environment by a single hydraulic cylinder. An alternative type of force control is achieved by creating a force on the environment which is directly related to the force that is exerted on the haptic device. This creates a good representation of the force exerted, especially for digging action, and would be the preferred switching solution for position control. A problem that arises in the case when feedback is given, when the bucket first comes in contact with the soil, the increase in gain produces instability problems [14]. A requirement for force control is the measurement of the end-effector, which is accomplished by the implementation of load pins at the joints[14], [11], [1] or pressure transducers [15].

Impedance control is a hybrid scheme, a combination of position control and force control. A typical example is what happens when the end-effector is moving in free space - the environment impedance is then set as low, while the control ( or master's) impedance is set as high. The control mode is then set in mode control for good trajectory tracking. If the environment is set to a high impedance - for example when digging - the controller is in mode and the control impedance is set to low. The slave acts as a force source/position sensor when in position mode, and as a position source/force sensor when in force mode, to minimise the effort while digging. The most relevant work is presented in [14], [11], [16], where the writers assume a constant slave environment impedance.

Several studies are also available on the electro-hydraulic control of earthmoving equipment [15], [14], [13]. Most of these studies were conducted by implementation of a control joystick and tele-operated tasks. Work conducted on the study of electro hydraulic control incorporated with a haptic device is found in Frankel et al [17]. Other relevant work includes Kontz et al [18]. The main objective of this literature is to receive

quantitative feedback, as well as to provide improvement in ease of control. Few studies have been done on the haptic device design input/as an excavator control input alone, the main goal being to improve training and to overcome the hurdle of inexperience.

For practical implementation a system model should be derived for the electrohydraulic control valves. The commercial value of the valves that were used in [17] is estimated at around \$1500 where, typically, four would be needed. Control and modelling of the valves is very difficult, and should be considered as a separate project. The main focus in [17] was to set up a test bed where further tests could be conducted on electrohydraulic control. As a parallel effort, mathematical models of the excavator were derived to provide both useful insight and a model that could be used for controller design [19]. The model is also used for real-time implementation to calculate endpoint estimation [16], force tracking [14] and dynamic representation for excavators under hydraulic control.

The excavator tasks and operations were studied, in order to compare them and derive the control algorithms. The kinematic relationships of the excavator joint angles and velocities, as well as torque, have been derived and are to be found in [20], [21], [22]. The notation was used to construct transformation matrices for each node relative to points in space. The kinematic relations and algorithm are fully derived and discussed in chapter 3. The next calculation of interest is the dynamics that relate applied forces to the resulting motions in the excavator's link. There are two modelling notations and both are well known and documented in [20], [23]. The first is Newton-Euler dynamic model based on  $\sum F = ma$  that relates the motion of one link to the next in a serial chain. The second is the LaGrangian dynamic model, based on the kinetic and potential energy. The LaGrangian model, which seems to be used in most of the literature [14], [24], is also the most computationally complex, but it provides the most intuitive insight into the dynamics.

To relate the predicted forces between the virtual environment and the haptic, several soil/rigid body models were reviewed in [11], [19]. There are several complex models available [25] but for most simulators

the model of the soil-bucket interaction forces are represented by a mass/spring/damper system. The main reason for using the spring-damper model is that a dynamic real time simulation of the digging forces acting on the end-effector is computationally very demanding. Thus, to create a more realistic real-time simulation for the haptic device implementation, the focus is shifted from the forces acting on the end-effectors to the feedback-forces that may be expected by the operator. The forces experienced by the operator serve as a warning, rather than reflecting the actual amount of force experienced by end effector. Several patents related to coordinated control have been released by several excavator and backhoe manufacturers. The most relevant are held by Caterpillar Inc [26], [27], [28], [29]. Others include Case [30], [31] and John Deere [32], [33] as well as Hitachi [34], [35], [36].

# Chapter 3

## Modelling

The purpose of this chapter is to provide the kinematic algorithms used to calculate the end-effector position when given the joint angle. The necessary inverse kinematic relations are also developed to relate the joint angles to the given end effector position. The four articulated links are labelled as the swing, boom, dipper and the bucket. The backhoe can be modelled as a four revolute joint serial-parallel mechanism, with the swing joint axis normal to the ground and the other three joint axes parallel to the ground [20].

### 3.1 Labelling convention and notation

The component frames and joint angles used throughout this work are illustrated in figure 3.2. The black dots represent the link origin and the pin joints, while the dashed lines represent the axes of the connecting frames. The link origins are represented by  $O_i$ . Scalar dimensions  $r_{x,y}$  are shown in italics, where  $x$  and  $y$  are the joint labels, eg the distance from point  $O_1$  to point C is given by  $r_{1C}$ . Angular quantities are given as  $\theta_{xyz}$ , where  $x, y$  and  $z$  are the points that describe the angle of the joint. The position vectors are indicated in the format  $\mathbf{p}^i$ , where  $\mathbf{p}^i$  is the position vector of the  $i^{th}$  coordinate frame  $\mathbf{p}^i = [x\ y\ z\ 1]^T$  (eg the bucket edge in the fourth coordinate frame is  $\mathbf{p}^4 = [0\ 0\ 0\ 1]^T$ ). A "1" is added to the

last element of the position vector to provide for the 4x4 transformation matrix in section 3.2, the convention adopted is thoroughly discussed in [20]. Matrix and vector quantities are shown in boldface format, with two dimensional vectors printed in uppercase and one dimensional column vectors in lower case. The following notation is also defined for the Denavit-Hartenberg (DH) transformation matrices,

$$c_1 = \cos(\theta_1) \quad (3.1.1)$$

$$c_2 = \cos(\theta_2) \quad (3.1.2)$$

$$c_{23} = \cos(\theta_2 + \theta_3) \quad (3.1.3)$$

$$c_{234} = \cos(\theta_2 + \theta_3 + \theta_4) \quad (3.1.4)$$

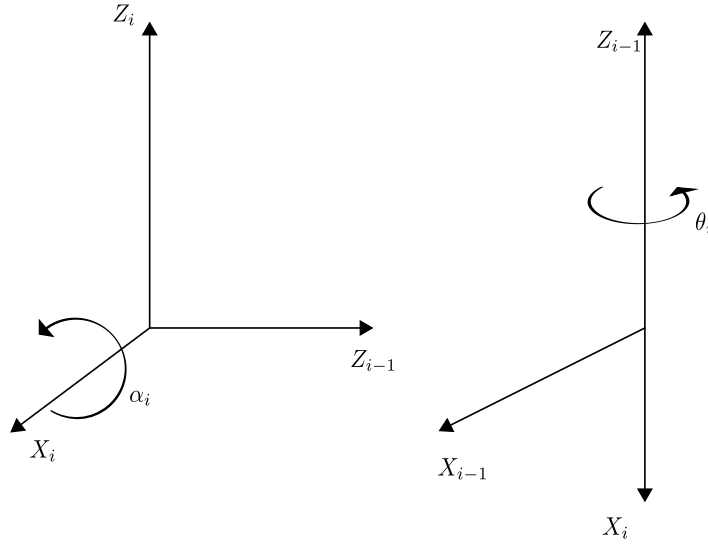
$$s_1 = \sin(\theta_1) \quad (3.1.5)$$

$$s_2 = \sin(\theta_2) \quad (3.1.6)$$

$$s_{23} = \sin(\theta_2 + \theta_3) \quad (3.1.7)$$

$$s_{234} = \sin(\theta_2 + \theta_3 + \theta_4) \quad (3.1.8)$$

- $\theta_i$ : angle between  $X_{i-1}$  and  $X_i$  measured about  $Z_{i-1}$  (see Figure 3.1),  $\theta_i$  is used if joint  $i$  is revolute
- $a_i$ : distance along  $X_i$  from  $O_i$  to the intersection of the  $X_i$  and  $Z_{i-1}$  axes
- $d_i$ : distance along  $Z_{i-1}$  from  $O_{i-1}$  to the intersection of the  $X_i$  and  $Z_{i-1}$  axes,  $d_i$  is variable if joint  $i$  is prismatic, and is thus 0 for excavator links
- $\alpha_i$ : angle between  $Z_{i-1}$  and  $Z_i$  measured about  $X_i$

Figure 3.1: Positive sense for  $\alpha_i$  and  $\theta_i$ 

### 3.2 Forward Kinematics

The Denavit-Hartenberg procedure is applied systematically to define the local coordinate systems for the serially connected links. The coordinate frames for the links are shown in figure 3.2, where the structural kinematic parameters which are presented in table 3.1 are defined. The link lengths  $a_i$  are measured from the origin  $O_{i-1}$  to  $O_i$  along the  $x_i$  axis, where the joint angles  $\theta_i$  are measured about  $z_{i-1}$ . For the structural kinematic parameters defined in table 3.1 the transformation matrices for rotational joints assume the following general form:

$$A_{i-1}^i = \begin{bmatrix} \cos \theta_i & -\cos \alpha_i \sin \theta_i & \sin \alpha_i \sin \theta_i & a_i \cos \theta_i \\ \sin \theta_i & \cos \alpha_i \cos \theta_i & -\cos \theta_i \sin \alpha_i & a_i \sin \theta_i \\ 0 & \sin \theta_i & \cos \alpha_i & d_i \\ 0 & 0 & 0 & 1 \end{bmatrix} \quad (3.2.1)$$

It follows then that position vector  $\mathbf{p}^i$  in the  $i^{\text{th}}$  coordinate system and

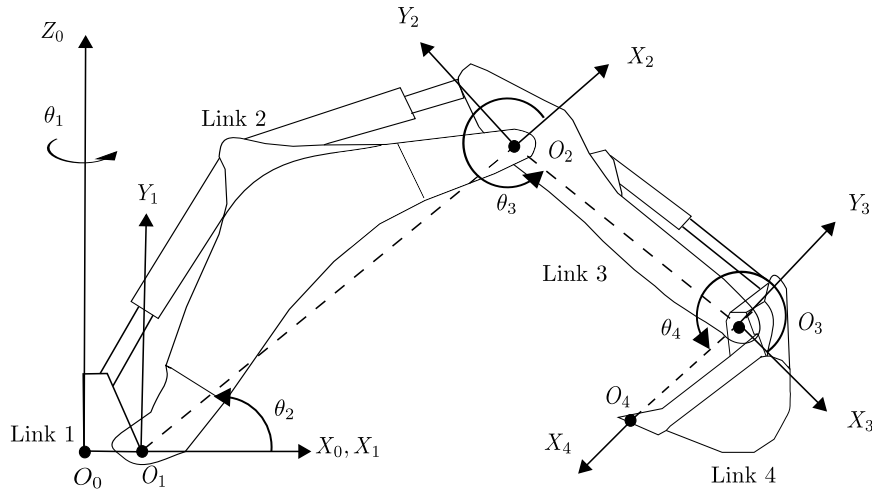


Figure 3.2: Excavator joint angles and component frames

Joint	Link lengths $a_i$	Joint angles $\theta_i$	Joint offsets $d_i$	Twist angles $\alpha_i$
1	0.05m	$\theta_1$	0	$90^\circ$
2	4.95m	$\theta_2$	0	0
3	38.7m	$\theta_3$	0	0
4	18.5m	$\theta_4$	0	0

Table 3.1: Denavit-Hartenberg parameters

vector  $\mathbf{p}^{i+1}$  in the  $(i + 1)^{th}$  coordinate frame are related by

$$\mathbf{p}^i = \mathbf{A}_i^{i+1}(\mathbf{p}^{i+1}) \quad (3.2.2)$$

Equation 3.2 can be used to relate vectors for the bucket position and orientation to those of the base. The fourth coordinate frame  $\mathbf{p}^4$  is related to the base coordinate  $\mathbf{p}^0$  frame as

$$\mathbf{p}_{04} = \mathbf{A}_0^4(\mathbf{p}^4) \quad (3.2.3)$$

where  $\mathbf{A}_0^4 = \mathbf{A}_0^1 \mathbf{A}_1^2 \mathbf{A}_2^3 \mathbf{A}_3^4$  and  $(\mathbf{A}_0^4)^{-1} = \mathbf{A}_4^0$ . The former transfer matrices for  $\mathbf{A}_0^4$  are calculated as follows:

$$\mathbf{A}_0^4 = \begin{bmatrix} c_1 c_{234} & -c_1 s_{234} & s_1 & c_1 a_4 c_{234} + c_1 a_3 c_{23} + c_1 a_2 c_2 + a_1 c_1 \\ s_1 c_{234} & -s_1 s_{234} & -c_1 & s_1 a_4 c_{234} + s_1 a_3 c_{23} + s_1 a_2 c_2 + a_1 s_1 \\ s_{234} & c_{234} & 0 & a_4 s_{234} + a_3 s_{23} + a_2 s_2 \\ 0 & 0 & 0 & 1 \end{bmatrix} \quad (3.2.4)$$

For the simulations the centre of the bucket edge is specified as  $\mathbf{p}^4 = [0001]^T$ . The bucket edge is thus related to the base coordinate as  $\mathbf{p}^0 = \mathbf{A}_0^4(\mathbf{p}^4)$ .

The bucket angle  $\phi$  is defined as the angle between the bucket ( $X_4$ ) and the ground plane  $X_0$ - $Y_0$ . The bucket angle is illustrated in figure 3.3, where a positive angle is defined as downward from the ground plane. The angle  $\phi$  will be used in the simulations to track the bucket angle relative to the ground or the desired path.

The bucket angle is calculated by defining the rotation matrix  $\mathbf{R}_4^0$  which can be interpreted as the projections of the base frame unit vectors onto the bucket frame unit vectors.

$$\mathbf{R}_4^0 = \begin{bmatrix} \mathbf{x}_0 \cdot \mathbf{x}_4 & \mathbf{x}_0 \cdot \mathbf{y}_4 & \mathbf{x}_0 \cdot \mathbf{z}_4 \\ \mathbf{y}_0 \cdot \mathbf{x}_4 & \mathbf{y}_0 \cdot \mathbf{y}_4 & \mathbf{y}_0 \cdot \mathbf{z}_4 \\ \mathbf{z}_0 \cdot \mathbf{x}_4 & \mathbf{z}_0 \cdot \mathbf{y}_4 & \mathbf{z}_0 \cdot \mathbf{z}_4 \end{bmatrix} \quad (3.2.5)$$

When the bucket position is calculated relative to the base frame, the angle  $\phi$  is found from the  $\mathbf{x}_4$  vector relative to the  $X_0$ - $Y_0$  plane. Since  $\mathbf{y}_1$

is always parallel to  $\mathbf{z}_0$  and  $\mathbf{x}_1$  is constrained to rotate in the  $\mathbf{x}_0\text{-}\mathbf{y}_0$  plane, the bucket angle is computed from

$$\phi = a \tan 2(\mathbf{y}_1 \cdot \mathbf{x}_4, \mathbf{x}_1 \cdot \mathbf{x}_4) + \pi \quad (3.2.6)$$

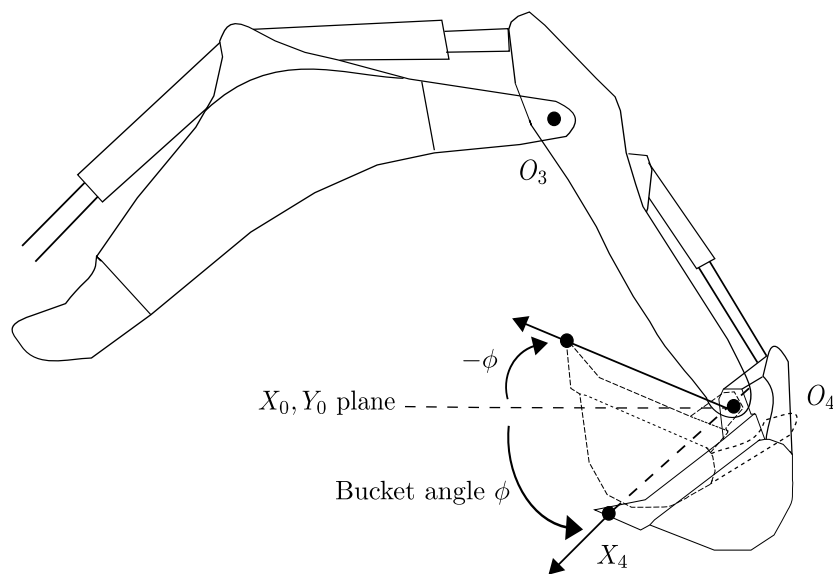


Figure 3.3: Illustration of the bucket angle

### 3.3 Inverse kinematics

The inverse kinematics are calculated to relate the joint angles for the given end-effector position. As mentioned in 4.1, the haptic device provides the dipper end position  $\mathbf{p}_0^3$ , while the control algorithm in 3.4 calculates the relative joint angles. The swing and bucket can be decoupled, as their angles are individually controlled by the wrist and trigger action.

The remaining two links (boom and dipper) form a planar arm where the joint angles are calculated as follows:

$$r_{13} = \sqrt{(r_{W_x})^2 + (r_{W_y})^2} \quad (3.3.1)$$

$$\theta_{31x_1} = \tan^{-1} \left( \frac{r_{W_y}}{r_{W_x}} \right) \quad (3.3.2)$$

where  $r_{13}$  is the distance from the  $O_1$  to  $O_3$  and  $\theta_{31x_1}$  is the angle between the points.

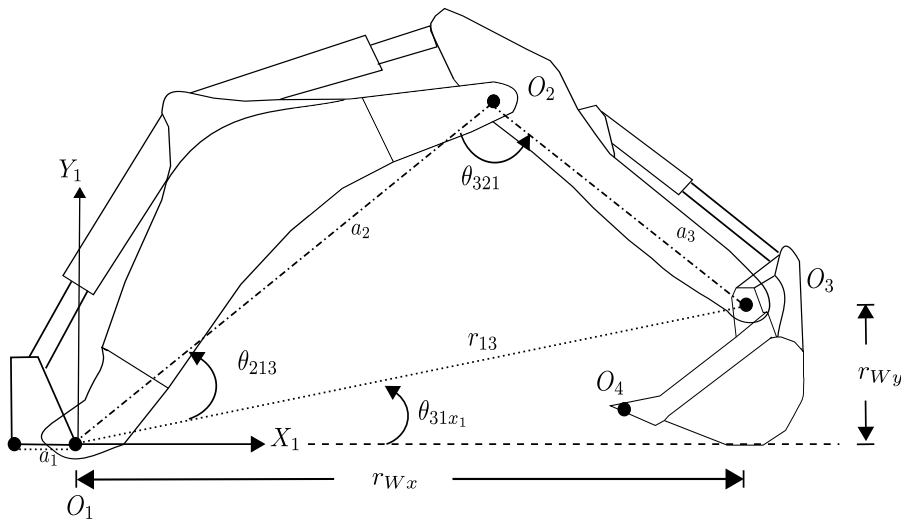


Figure 3.4: Excavator joint angles and component frames for inverse kinematics

The inner angles can then be found by using the cosine law,

$$\theta_{321} = \cos^{-1} \left( \frac{a_2^2 - r_{13}^2 + a_3^2}{2a_2a_3} \right) \quad (3.3.3)$$

$$\theta_{213} = \cos^{-1} \left( \frac{a_2^2 - a_3^2 + r_{13}^2}{2a_2r_{13}} \right) \quad (3.3.4)$$

the angles  $\theta_2$  and  $\theta_3$  can then be calculated from

$$\theta_2 = \theta_{213} + \theta_{31x_1} \quad (3.3.5)$$

$$\theta_3 = \theta_{321} + \pi \quad (3.3.6)$$

### 3.4 Summary

Using equations 3.3.1 to 3.3.6 the joint angles can be calculated with the given bucket orientation. The forward kinematic relations of the joint angles are also calculated, to track the end effector. Restrictions have been placed on the joint angles which are directly related to restrictions on the actuator links. The kinematics relations derived in this chapter are used to simulate and/or control the excavator, the inverse kinematics being related more to control and the forward kinematics to the measurement and simulation.

# Chapter 4

## Design and construction

This chapter describes the concept and the detailed design and construction of the haptic device. The first step was to determine the required degrees of freedom necessary for the haptic device to control the excavator. The initial idea was to construct a joystick/robotic arm with multiple links that resembled the actuator links of an excavator. This concept had previously been implemented and several patents are available [37]. Two main problems could arise from this configuration, depending on the method of control used (position or rate). If position control is used the user could become fatigued by the constant extensive arm movements and stress could be placed on the operator's joints. With rate control, or a combination of rate and position, the angles of the joystick links do not coincide with the angle orientation of the excavator links, which could confuse or frustrate the operator.

### 4.1 Concept design

The following design criteria and requirements were considered after comparing the haptic devices available with the general requirements for haptic devices.

- The design of the haptic device should be robust enough for the excavator or backhoe operator environment.

- The haptic device should be able to provide sufficient feedback, and the operator should be able to distinguish between machine vibration and haptic feedback.
- The workspace should be small but efficient, in order to allow the implementation of several control methods whilst keeping the correct ergonomic aspects, i.e high force and position bandwidth.
- The haptic device should be intuitively orientated with relation to the excavator actuators, eg rotating wrist action should cause the boom to swing in the rotated direction.
- The haptic device should not mechanically limit the user's movement or actions, and it should prevent the master (haptic device) from inducing an actuator lag.
- The haptic device should not have any mechanical play and should produce smooth motions with low inertia.

The solution, and the intention of the project, is to create an ergonomic single input device that relates all the joint positions to a single end-effector point. The concept design is illustrated in figure 4.1, where all the input actions are numbered. The dipper end position is controlled by specifying the Z and X coordinates with the downward (2) and forward (1) control motions. The swing is controlled by the wrist action (3) while the bucket is then separately controlled via the trigger (4). Figure 4.2 illustrates the input actions related to the excavator link movements. The degrees of freedom and movement are also illustrated in figure 4.1 and listed in table 4.1. From figure 4.2 it may be noted that the user will have the ability to move the end of the dipper in a smooth horizontal line (1).

A combination of rate and position control is used. The actuator regions are divided into smaller regions, where the user moves between the control schemes. To illustrate the control scheme, the control regions for the linear actuator are indicated in figure 4.1. If the operator wanted to perform small precise movements he would position the actuator in

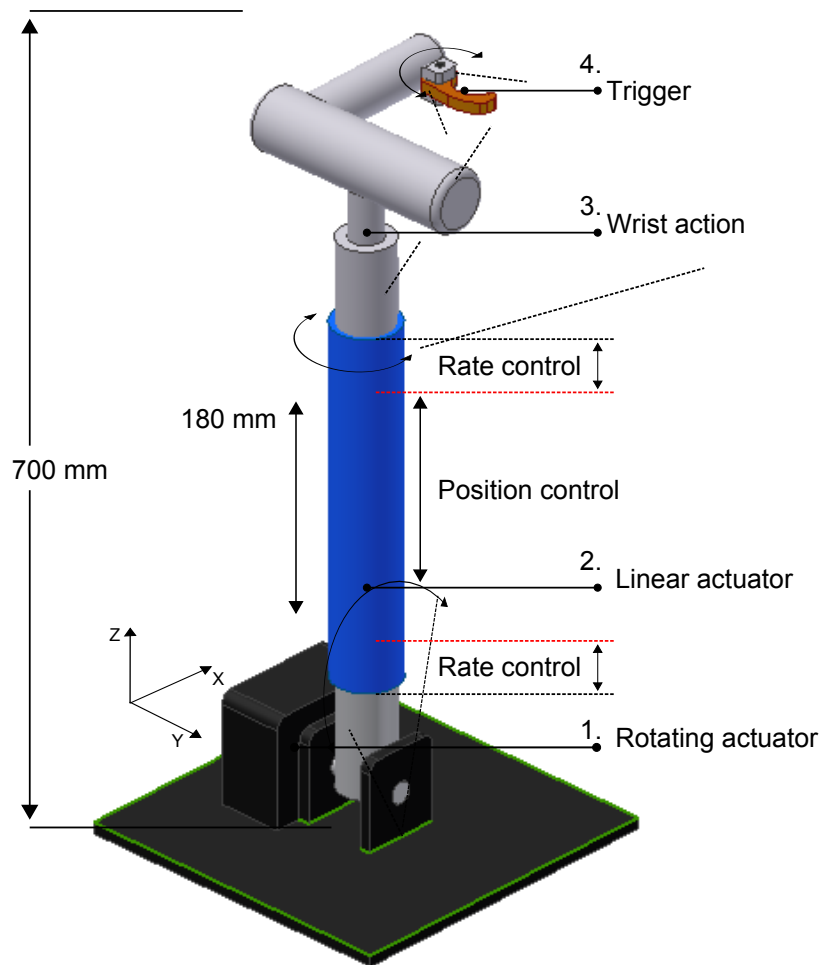


Figure 4.1: Concept design of haptic device

the position mode region, whereas if he wanted to perform a large control movement he would position the actuator in the rate region.

Another way of describing the control method is by the imagining a small blocked area around the actuated link, as illustrated in figure 4.3. The inner part of the block represents the position region of the haptic device, where the dipper end-effector position in the block is directly related to the haptic device position in the position region. If the haptic device is moved in the rate region, further from the centre of the block, the dipper end-effector will move at a rate related to the input position in

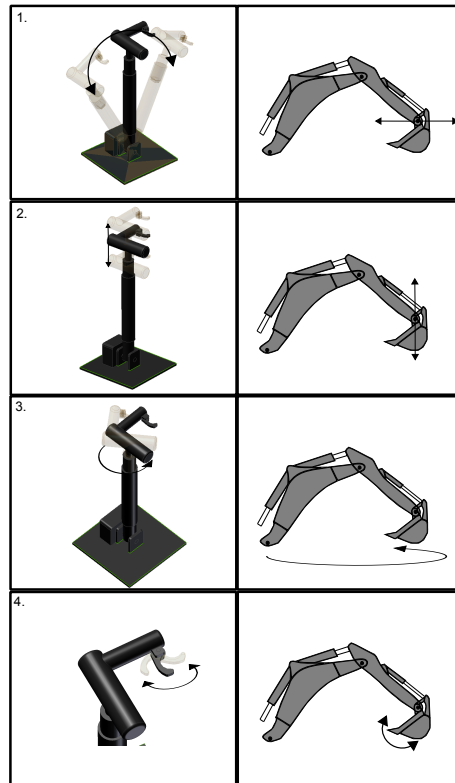


Figure 4.2: Illustration of control scheme

the rate region (the closer to the rate limit the greater the rate of change). Also, when the input is in the rate region, the upper limit of the box changes or moves with the dipper end-effector until the haptic device is positioned back in the position region.

Each haptic device control movement is positioned by actuators described in the subsections below. Two main types of actuators are commercially available, hydraulic and electro-mechanical. Hydraulic actuators are expensive and require an external hydraulic pump. An electro-mechanical actuator setup from Festo, with similar dimensions to that of the actuator in figure 4.5, would cost well over R5000-00. The biggest

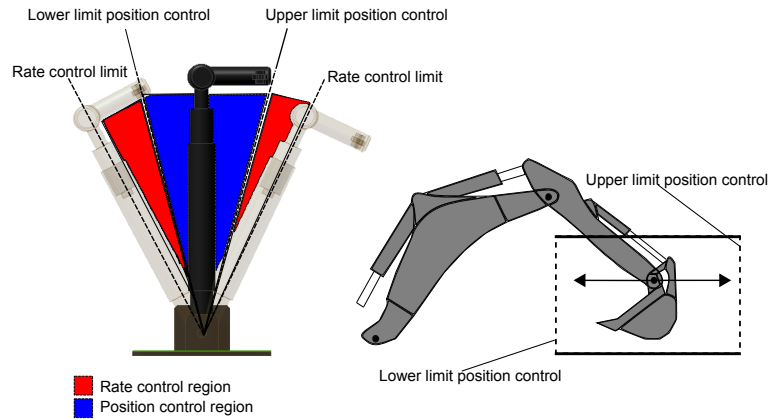


Figure 4.3: Illustration of control scheme and regions

Movement	Actuator	Input range	Position control	Rate control
1	Wrist	44°	± 11°	± (11:22.5)°
2	Rotation	75°	± 25°	± (25:37.5)°
3	Linear	160mm	± 62.5mm	± (62.5-80)mm
4	Trigger	90°	± 22.5°	± (22.5:45)°

Table 4.1: Workspace and control regions of actuators

problem with the actuators available is the speed and feed force relationship. The actuator from Festo performed at the desired actuator speed of 0.5m/s but produced a feed force of 300N. The solution was to build actuators using basic geared direct current (DC) motors with the ability to produce the desired feedback as regards both frequency and force. The implementation of a DC motor as a force reflecting actuator is sufficient [38]. The two main input factors of interest are the actuator position and the force applied by the user. The force is measured by a strain gauge and the position by a linear potentiometer (POT). The resolution of a POT is sufficient, as it has a smaller resolution than the human finger, wrist and elbow [39]. The applied force controls the actuator position to produce a smooth action, and this is a requisite as two main actuators are geared and cannot be moved freely. The solution was to sense the force applied by the operator and produce the desired haptic device movement with

the actuator whilst measuring the position with a POT. A typical example of this is when the operator wants to move the end-effector to the ground; he applies a downward force to the haptic device, where the force is then measured by the strain gauge. The actuator then moves in the direction of the applied force with a speed relative to the magnitude of the force, whilst the POT measures the position.

## 4.2 Detailed mechanical design

To fulfil the design requirements for the haptic device using the aforementioned control scheme, the following minimum actuator requirements were derived in terms of speed and force output.

- The minimum actuator speed was calculated using the average end-effector speed of a professional operator (0.5m/s) [40]. By comparing the workspace of the excavator and that of the haptic device, the minimum required actuator speed is calculated as 0.01m/s. The actuator should be as fast as possible whilst still providing sufficient feedback.
- The actuators should be able to produce minimum feedback force of at least 7N, which is 1.4 times greater than the current feedback of the haptic devices [18] known to have been implemented.

### 4.2.1 Rotation actuator

The rotation actuator acts as the pivot point for the haptic lever illustrated in figure 4.4. The load is sensed via a strain gauge which was calibrated to produce the output in table 4.4. The actuator implemented was a DC motor, i.e a wiper motor with the specifications given in table 4.2.

The DC motor was controlled via the H-bridge motor driver discussed in 4.3.1. The wiper motor option was chosen as it was the best priced, compared to other commercial high torque DC motors with the same

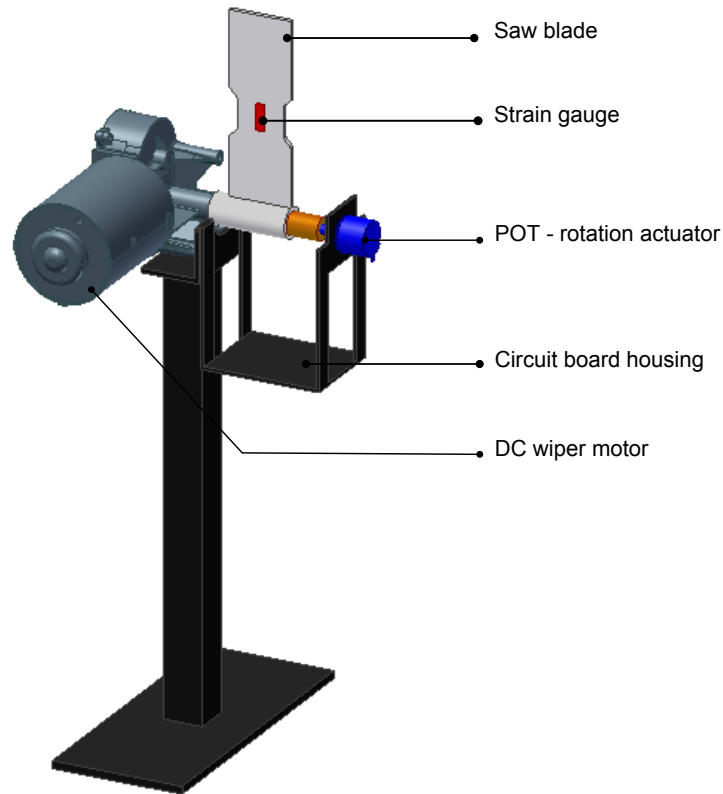


Figure 4.4: Rotation actuator

RPM, for the purpose of fulfilling the design requirements in respect of frequency and feedback.

Supply Voltage	Stall Torque	RPM	No Load current	Stall current
12 V	9.4 N.m	60	1.53 A	5.3 A

Table 4.2: DC motor characteristics of the rotation actuator

### 4.2.2 Linear actuator

Electrical linear actuators are very expensive. The desired linear actuator should produce a minimum feedback force of 7N with the handle grip

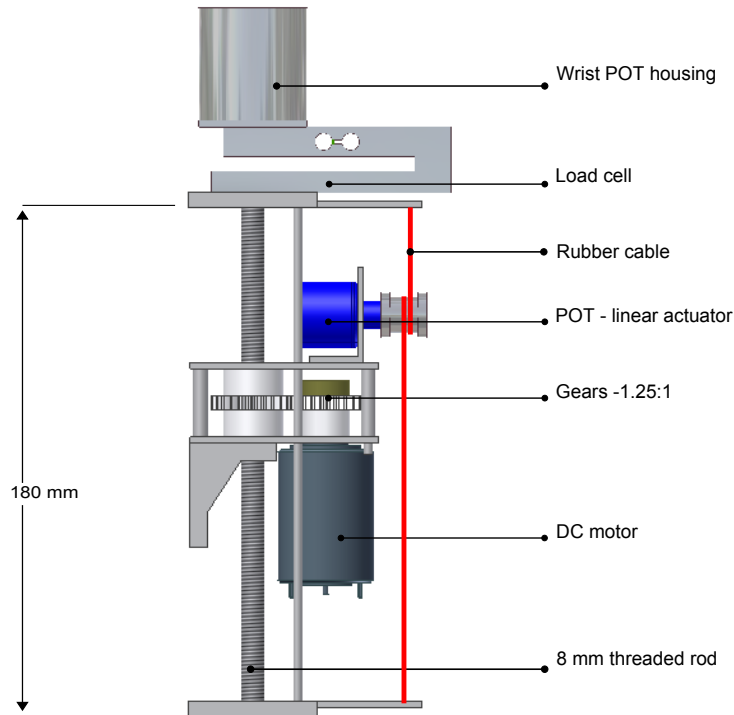


Figure 4.5: Linear actuator

of 620g fitted. The linear actuator should be able to produce a linear movement greater than 0.01m/s. The solution for the linear actuator was to extend a threaded rod by rotating a threaded gear via a DC motor, extending and retracting as the motor rotated in the desired direction. The torque ( $T_R$ ) required of the DC motor to produce the desired force ( $F$ ) is given by Joseph et al. [41] as,

$$T_R = \frac{Fd_m}{2} \left( \frac{l + \pi f d_m}{\pi d_m - fl} \right) \quad (4.2.1)$$

In the above equation,  $d_m$  is die screw diameter (8mm),  $l$  is die screw pitch (2mm) and  $f$  is the friction coefficient (0.08) between the threaded gear and actuator rod [41]. From equation 4.2.1 it was calculated that a torque of 8.4mN.m was required by the DC motor.

Supply Voltage	Stall Torque	RPM@85 mNm	No Load current	Stall current
12V	0.101 Nm	5000	2.58A	13.2A

Table 4.3: DC motor characteristics of the linear actuator

The required motor speed [rev/s] was calculated as follows,

$$M_s = V_l / l \quad (4.2.2)$$

where  $V_l$  is the actuator speed of 0.01m/s and  $l$  is the mechanical screw thread pitch (2mm). The motor implemented was a heavy duty 12V DC motor from Johnsen motors which is typically used in hand held vacuum cleaners and printers. The DC motor specifications are tabulated in table 4.3. To ensure sufficient torque, taking into account friction losses and motor efficiency, a gear ratio of 1.25:1 was also implemented.

The linear actuator constructed is illustrated in figure 4.5. A practical force output of 14.7N and an actuator speed of 0.16m/s was obtained with the handle grip fitted. Because of friction and motor inefficiency, these are much lower than the estimated values calculated by equation 4.2.1 and 4.2.2. The force applied by the operator in the downward direction is measured by the load cell. A load cell was used because it resulted in sufficient accuracy and it isolated the forces applied by the operator in the Z axis.

### 4.2.3 Wrist and bucket action

The wrist and trigger action applied by the operator are measured by a POT. The wrist action is directly related to the excavator's swing action i.e rotating the grip-handle to the left produces a swing action in the same direction. The bucket is closed by pulling the trigger towards the operator and opened by pushing the trigger away. The trigger was positioned and designed to give the operator the freedom of controlling the trigger with his thumb for greater comfort and accuracy.

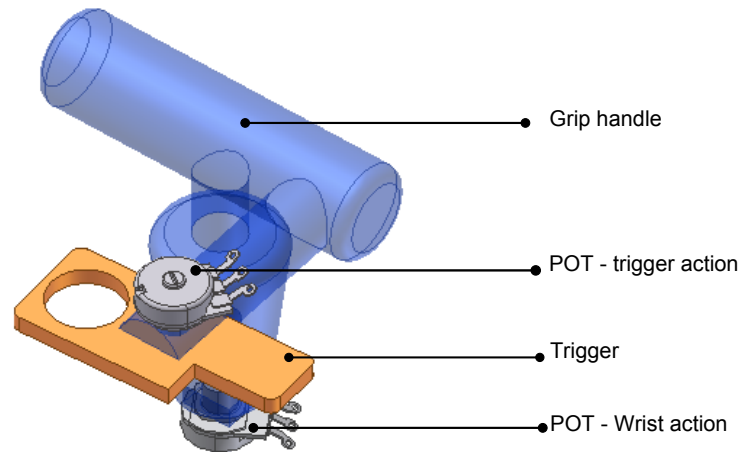


Figure 4.6: Wrist and trigger

### 4.3 Motor controller design

Both DC motors were supplied with 12V via two separate voltage supplies. The motor controller design consisted of four major components which are illustrated in figure 4.7. The dsPIC samples the filtered input signals from the strain gauge amplifiers and then adjusts the duty cycle of the pulse width modulated (PWM) signal accordingly. A full bridge design was implemented to control the direction and speed of the DC motor and this is illustrated in figure 4.8.

The following design criteria were considered for the H-bridge design: It should

- be able to handle a maximum continuous motor current of at least 15A.
- handle supply voltages up to and including 15V.
- provide the ability to adjust motor switching characteristics.
- shut down the motor if necessary.
- provide switch protection as well as shoot-through prevention.

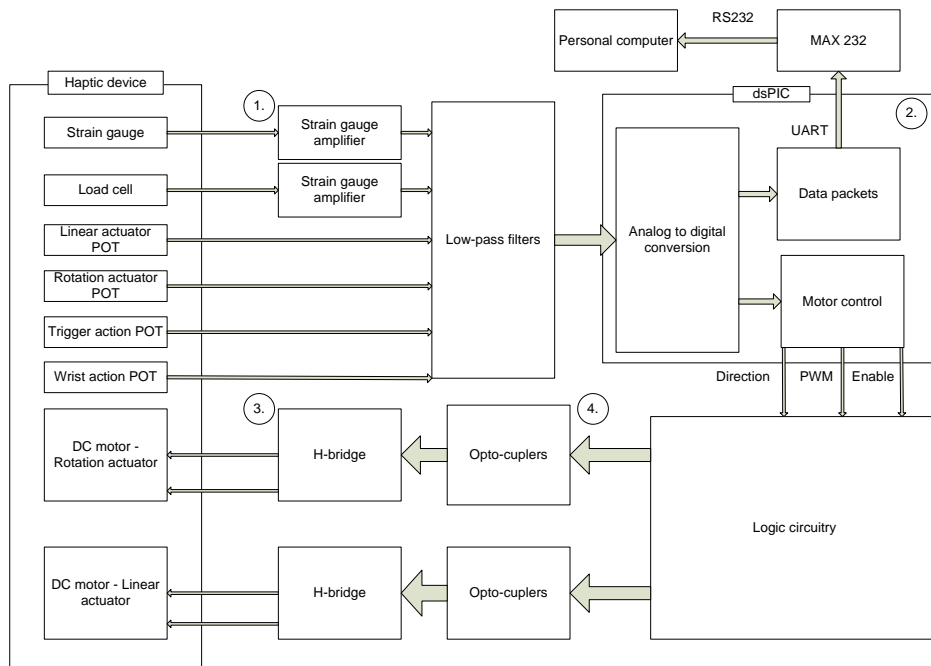


Figure 4.7: Conceptual overview of motor controller

- be versatile and have the ability to be implemented on both DC motors used.
- be power efficient, keeping switching losses to a minimum.

For the switch selection MOSFETs were used, as they were cheaper than IGBTs while still having a low voltage drop. The IRF540 MOSFET that was implemented had a maximum current rating of 33A and on resistance of  $44\text{m}\Omega$ .

The two main factors that were considered with MOSFET driver choice were the voltage transition and MOSFET protection. The switching signal to the MOSFET gate should be clean to provide a fast transition between high and low, and for MOSFET protection no shoot-through voltage should occur on the bridge.

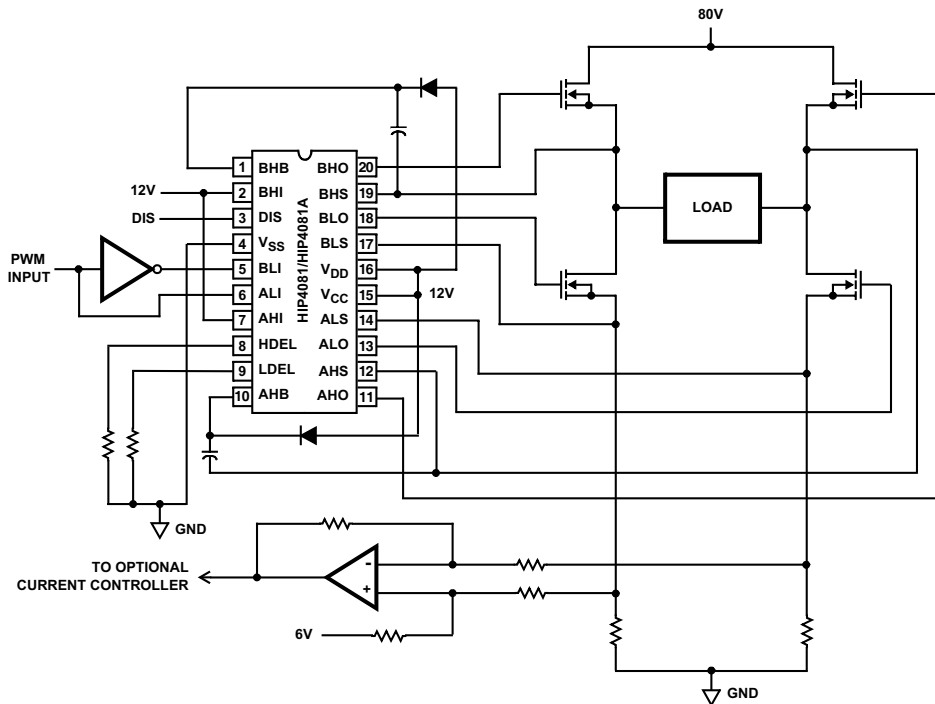


Figure 4.8: Application diagram of the H-bridge

### 4.3.1 MOSFET driver

The HIP4081A MOSFET driver from Intersil was used; the design alternative was the IR2110 half-bridge driver from International rectifier. The main advantage of the full-bridge HIP package over the IR2110 was synchronisation. Two half-bridge chips would be needed for a single motor controller, requiring more control pins and thus increasing complexity by requiring protection and gate drive considerations.

The HIP4081A chip includes under-voltage protection, adjustable dead time controller and a disable pin. Each leg of the H-bridge is individually controlled by the assigned input pins, where shoot-through protection is included.

### 4.3.2 Strain gauge amplifiers

A simplified diagram of the strain gauge amplifier constructed is illustrated in figure 4.9. The strain gauge amplifier uses the Wheatstone bridge to calculate the change in resistance. Due to different resistance values and material characteristics, two separate amplifiers were constructed, one for the load cell and the other for the strain gauge (rotation actuator). The INA128 instrumentation amplifier from Texas Instruments was implemented, which is typically used in applications such as bridge amplifiers and thermocouple amplifiers. The circuit recommended in the data sheet was implemented for the bridge amplifier. The INA128p delivers gain of up to 50000 by changing the  $R_G$  value in figure 4.9, where  $R_S$  represents the strain gauge. The load cell uses two  $1000\Omega$  strain gauges doubling the sensitivity. The calibration and output for the load cell and strain gauge are illustrated in table 4.4, where the force input range relates to the force applied to the handle grip in a single direction i.e forward or downward. The output of the strain gauge lies between 0 and 5V, and is 0 when no force is applied to the handle.

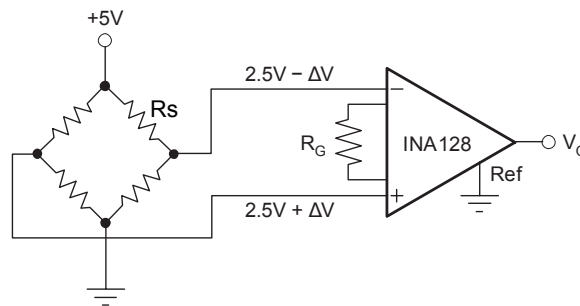


Figure 4.9: Simplified circuit diagram of strain gauge amplifier

### 4.3.3 Opto-couplers

To protect the dsPIC micro controller and to prevent noise from entering the strain gauge amplifiers, Opto-isolators were used to connect the mo-

	Resistance ( $\Omega$ )	Amp gain	Input range [N]	Output [V]
Strain gauge	120	1786	1.2-14.7	0-5
Load cell	1000	2273	1.2-14.7	0-5

Table 4.4: Strain gauge comparison and output relative to force input

tor control signal to the H-bridge circuit. The choice of the opto-isolators was not that critical, the main requirement being that it should be able to handle a PWM frequency of 30kHz. The MCT2E was implemented because of availability and because it fulfilled the design requirements.

#### 4.3.4 dsPIC controller

The dsPIC30F4011 micro controller from Microchip was implemented, being part of their motor controller family. The dsPIC30F4011 was chosen because of its operating frequency, motor control, PWM capabilities and UART. The microcontroller was programmed via Microchip's IDE programmer, implementing the C compiler as programming language. One of the other main reasons for implementing the dsPIC30F4011 was the number of input and output pins for multiple input sampling and dual PWM control. The dsPIC30F4011 provides 8 inputs for the on board 10bit analog to digital converter, while only 6 were required by the haptic device.

The motor control actions taken to control the rotation actuator is illustrated in figure 4.10. Dead-band is inserted due to the torque applied by the linear actuator and grip handle weight, which changes the sensitivity of the strain gauge. The upper and lower dead-band is calculated according to the POT position. The actuator is then moved in relation to the strain gauge input.

## 4.4 Summary and final design

This chapter has provided a high level discussion of the hardware related to the construction of the haptic device. The fully constructed haptic de-

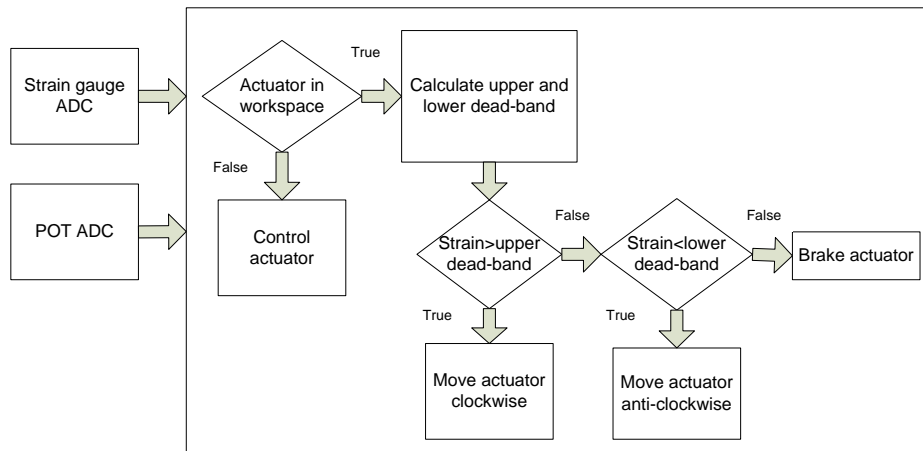


Figure 4.10: Calculation steps taken with motor control

vice is illustrated in figure 4.11. The haptic design dimensions are presented in appendix B, with the hardware details in appendix C. The next step would be to test the control by connecting it to the virtual excavator simulator discussed in chapter 5. 5

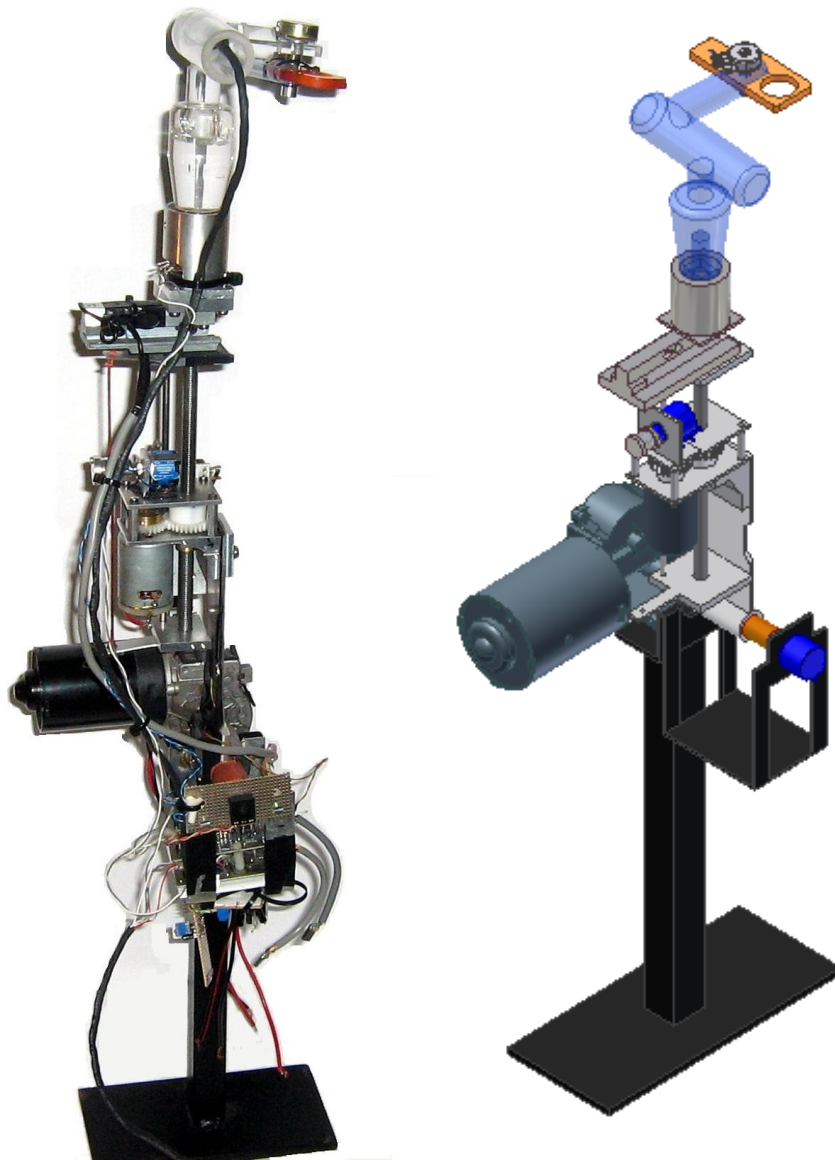


Figure 4.11: Illustration of the constructed haptic device - actual haptic on the left and the CAD model on the right

# Chapter 5

## Virtual excavator and simulator software

This chapter describes the simulation on the system evaluation software.

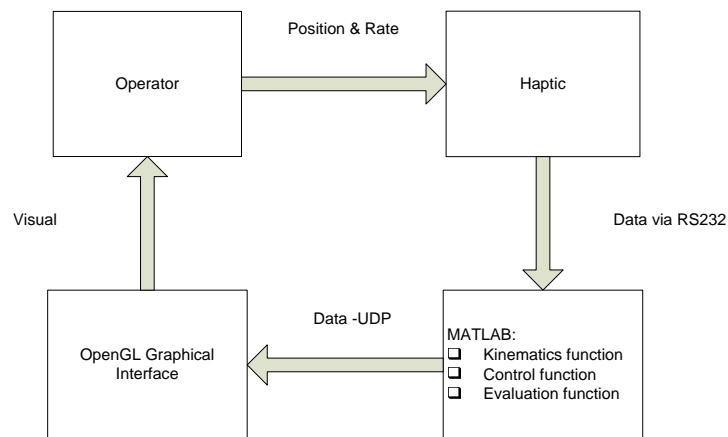


Figure 5.1: Interaction of software modules

The simulator consists of several software modules interacting, as illustrated in figure 5.1, where each module is discussed in the following subsections. The purpose of the simulator was to construct a graphical interface to test and compare the ergonomic efficiency and the task

efficiency of the joystick and the haptic device. The first step was to create a basic excavator simulator controlled by two joysticks, with the orientation as shown in figure 1.1. Logitech Attack 3 joysticks were used, as they had the same control orientation and physical aspects as the joysticks implemented in almost all excavators nowadays. Test subjects would be asked to perform certain tasks on both input setups (joysticks and haptic device). These tasks and the results obtained are discussed in chapter in 6. An experienced operator was asked to validate the simulator with regard to joystick orientation as well as the general movement of the excavator. For greater realism, the speed of the actuator joints was simulated according to the hydraulic speed given in the operator's service manual of a Kamatsu WB91-2 backhoe.

## 5.1 Graphical interface

The graphical interface was developed in QT, which is a cross-platform application framework. Graphical interfaces and applications developed in QT can be deployed across many desktop and embedded operating systems without rewriting the source code. QT uses C++ with several non-standard extensions implemented by an additional pre-processor that generates standard C++ code before compilation. The main block-sets and functions used in QT are illustrated in figure 5.2 and discussed in the following sections. QT was chosen, because of being open source and well documented, providing numerous demo examples. The other main reason was that it provided the standard OpenGL widget, enabling OpenGL rendering.

### 5.1.1 GLwidget

QT provides the GLWidget class to enable OpenGL graphics to be rendered within a standard application user interface. By subclassing this class, and providing reimplementations of event handler functions, 3D scenes can be displayed by widgets that can be placed in layouts, con-

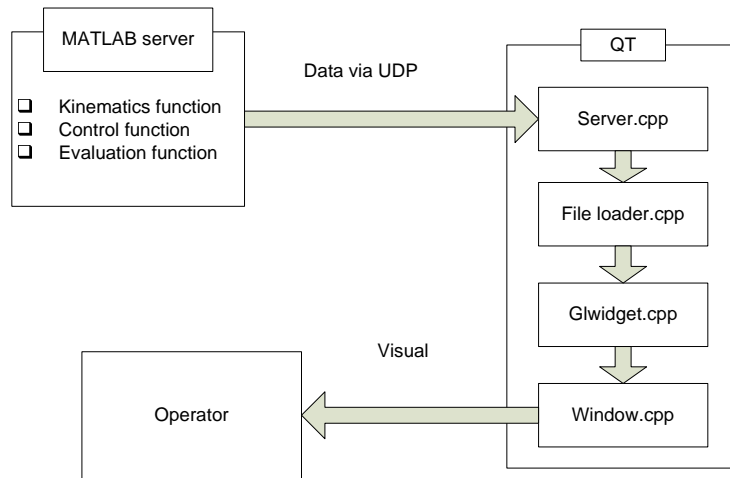


Figure 5.2: Block sets and functions

nected to other objects using signals and slots, and manipulated like any other widget. In the case of widgets that needed only to be decorated with pure OpenGL, the `paintGL` function is used to paint the contents of the scene onto the widget. The main objects that were rendered in the `GLwidget` were the 3D world and the excavator arms, as well as the target-points and line traces. The objects, in `.3DS` format, are loaded into the scene via the file loader developed by Busch [42].

One of the advantages of the OpenGL rendering is that the model view and projection of each object is stored as a matrix stack. By manipulating the matrix stacks via the `glPushMatrix()` and `glPopMatrix()` commands, the objects rendered can be rotated and translated according to the previous matrix stack. Therefore no calculated transformation matrices were needed to render and perform the visual rotation of the excavator joints.

The `glPushMatrix()` matrix command copies the current matrix and adds the copy to the top of the stack, while `glPopMatrix()` discards the top matrix on the stack. The typical procedure for the boom and dipper rendering would be to call the `glPushMatrix()` command (where the base matrix was the previous stack), rotating the boom  $\theta_2$  according to

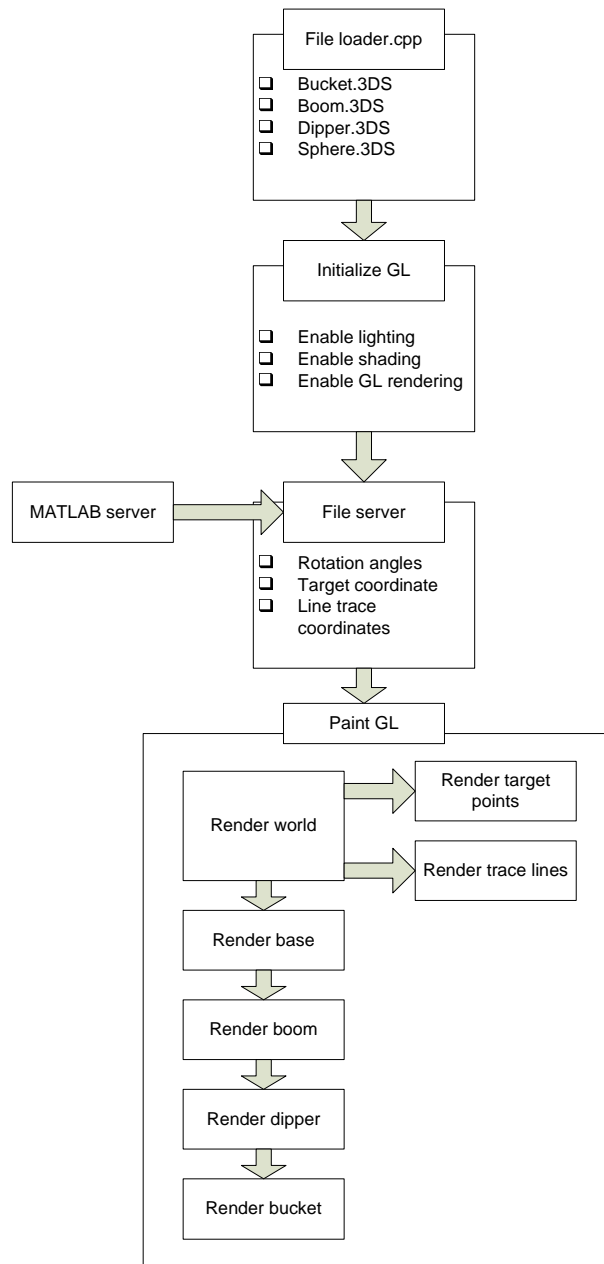


Figure 5.3: Block diagram of the GLwidget class

the previous stack  $\theta_1$ . In effect, the `glPushMatrix()` and `glPopMatrix()` commands could be seen as switching between the axes (0-4), where the rotation and translation occurring after the `glPushMatrix()` command is

relative to the previous axes (matrix stack). The main steps followed in the GLwidget class are illustrated in figure 5.3.

### 5.1.2 Window

The window contains the openGL that is rendered and constructs a graphical user interface which gives the user the ability to add tabs and slider bars etc. For the sake of simplicity, and to allow the user to freely rotate the camera angle, 4 slider bars are added on the right, which control the point of view. Figure 5.4 illustrates the window output screen and the slider bars.

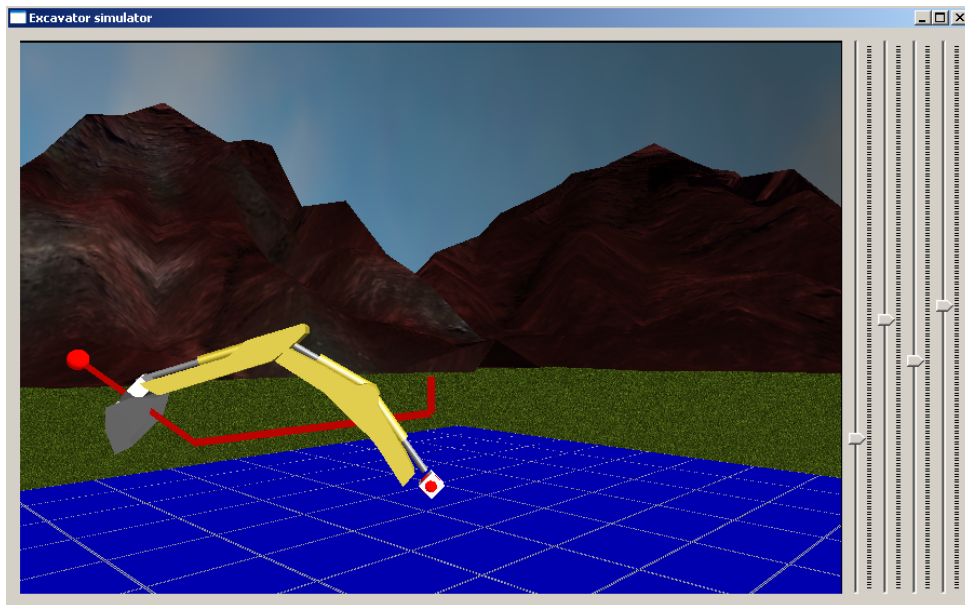


Figure 5.4: Graphical interface with a side view of the excavator links

### 5.1.3 Network server

The server developed by Busch [42] is implemented for communication, receiving data packets from MATLAB, updating the specified variables in the QT environment. The network protocol implemented was UDP,

where the data transferred is defined as packets. The main data packets sent via the server are listed in the server block in figure 5.3.

### 5.1.4 File loader

The file loader module is used to load the external 3DS files. The lib3ds library is used by the file loader to manage the .3DS file format. The file loader allows the import of the basic model and scene data, which is listed in [42].

## 5.2 MATLAB simulation

The main software blocks used in MATLAB are illustrated in figure 5.5. The excavator joint angle output is connected via the MATLAB server s-function and displays the calculated angles and the interaction of the excavator’s end-effector with the target objects.

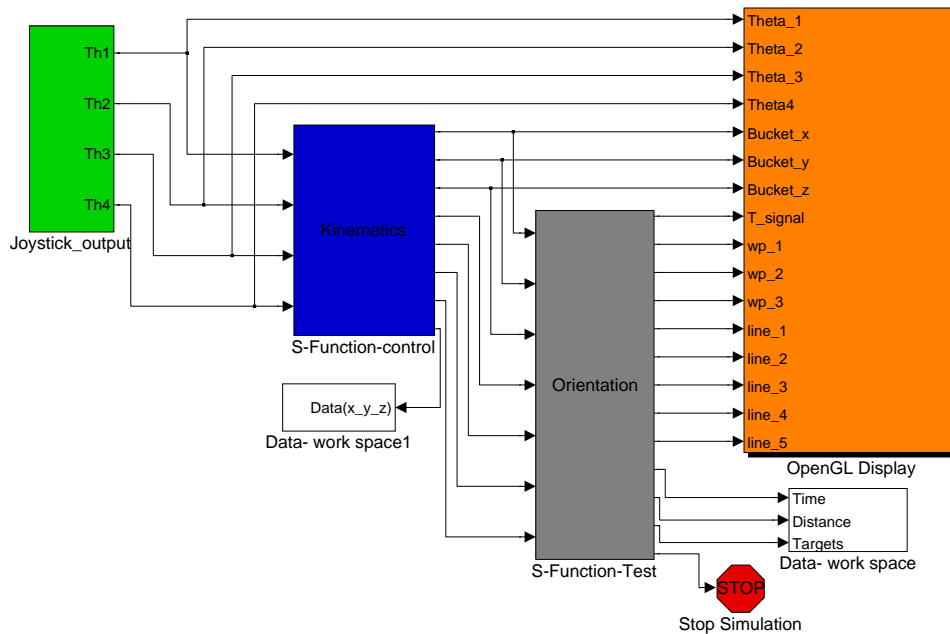


Figure 5.5: MATLAB simulink model with excavation block

### 5.2.1 Input functions

The main functions used to control the input device can be divided into two parts; the serial input s-function and joystick input block. The serial input function is used for the haptic device tests, while the joystick (USB) is used for the joystick orientation.

#### Serial-port input

The main function of the serial-input block is to open the specified COM port at the specified communication speed (115200bps). The serial-block receives the data packets from the dsPIC at the specified sample interval (0.02s) and then reassigns each data packet to a specific output port.

#### AeroSim - Joystick block set

The joystick block-set was obtained from the AeroSim toolbox that was developed by Unmanned Dynamics, which is freely available to all academic and non-commercial users. The joystick block output was calibrated for the Attack 3 joystick.

### 5.2.2 Input control and kinematics

The control and kinematic block relates the output of the input function to the angles of each link. The angles are calculated by using the input setup illustrated in fig 4.1, the angles increasing at a rate of change relative to the position of the joystick. The position of the end effector is calculated and then passed on to the work space and the required test block. Limits are also applied for each link, in order to create the effect of greater realism. The end effector is limited, allowing the operator to work only above the ground plane, preventing awkward, unrealistic link orientation.

### 5.2.3 MATLAB client

The OpenGL block illustrated in 5.5, which allows up to 32 inputs, was developed by Busch [42]. The block communicates via UDP to the OpenGL interface discussed in 5.1. The main inputs to the OpenGL block are the link angles and the test signals relative to each evaluation block.

### 5.2.4 Evaluation block sets

The two variables of greatest interest for evaluation were distance and time. Four block-sets were developed, each to test a specific ability of an inexperienced operator relating to the control input setup (haptic device or joystick). The blocks calculate the variables desired and write the array of variables to the workspace, to be saved and compared. After all the operators have completed the tests, the average of the data for each test is written to an Excel spreadsheet. The Excel spreadsheet is then used to plot, compare and analyse the results of all the operators.

#### Orientation block

The Orientation block was created to provide an initial test and to familiarise the user with the input device and the input control. This block produces target point coordinates through which the user has to pass with the smallest amount of effort and as quickly as possible. The main steps of the orientation block calculation are illustrated in figure 5.6. The block tracks the total distance travelled by the end effector, as well as the minimum distance between the target points.

#### Trace block

The trace block produces a path which the operator has to follow as closely as possible, where the starting point of the trace line is indicated by a red sphere. The trace simulation is illustrated in section 6.2. The block produces the start and end points of all the vertices drawn in the OpenGL module. The difference in distance between the desired path

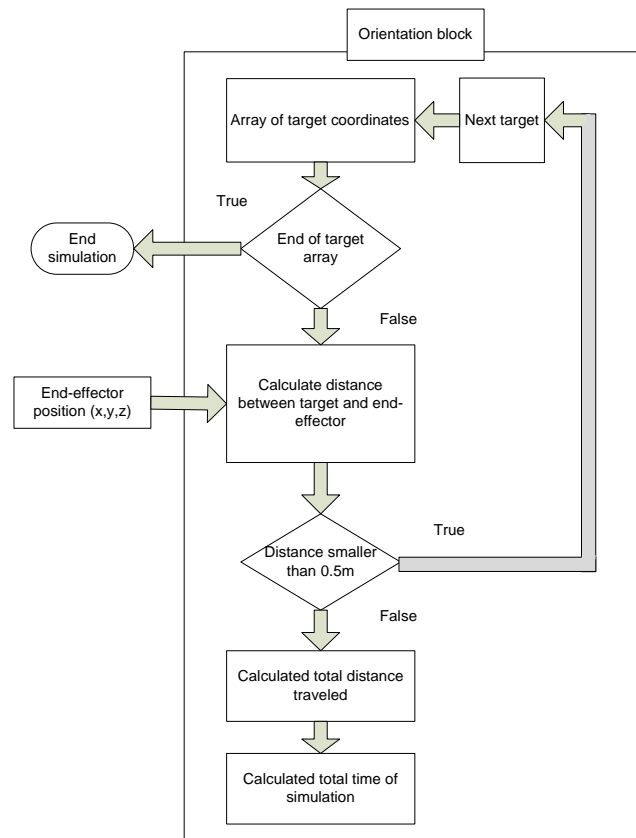


Figure 5.6: Calculation steps of Orientation block

and that of the end effector, as well as time taken, are calculated and sent to the workspace. The main steps of the trace block calculation are illustrated in figure 5.7.

### Grade block

The grade block tests the operator's ability to keep the bucket height, as well as the bucket angle, constant for a specified path. Grading is performed after an excavation to scrape, level or trim uneven spots for final smoothing and levelling. Grading is classified as a difficult task, and is only executed efficiently by professionals.

The grade block starts measuring the data (bucket angle and height) once the end effector passes through the starting point, which is indi-

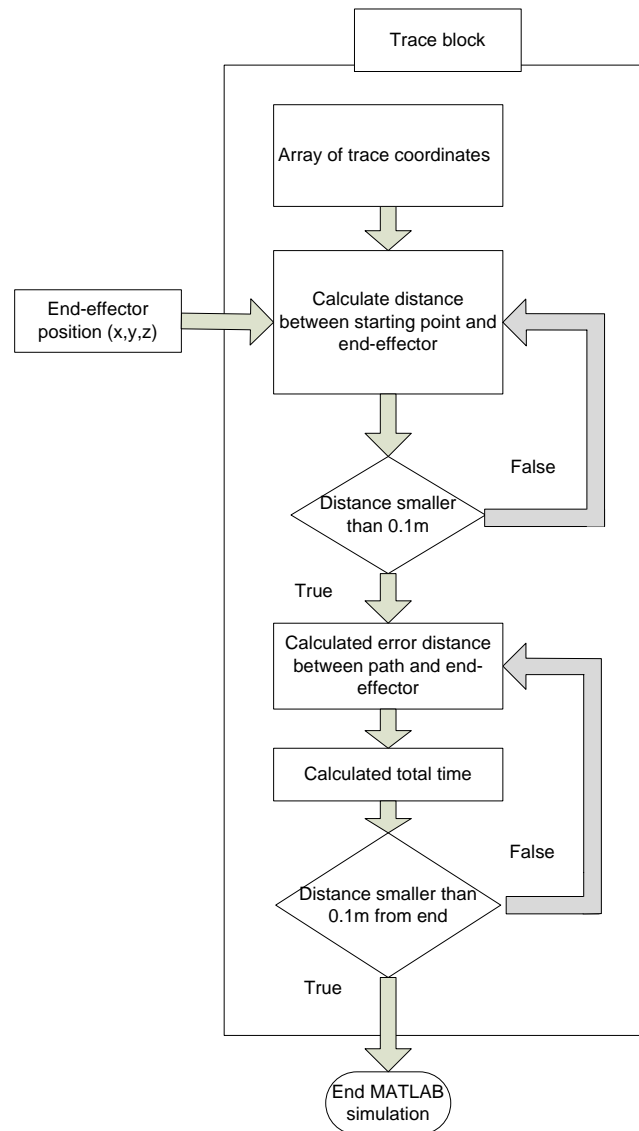


Figure 5.7: Calculation steps of Trace block

cated by a red sphere. Any error in bucket angle is calculated by subtracting the current angle from the angle desired. The error in height is calculated similarly. The main steps of the grade block calculation are illustrated in figure 5.8.

**Excavation block**

The excavation block generates a ball that can be moved around, enabling the user to pick the ball up and drop it at a desired location. The picking up and dropping of the ball simulates the digging action of an excavator, requiring the same input sequence.

The excavation block calculates the direction vector of the end-effector and then translates the ball in the same direction. The block also calculates the bucket angle and orientation required to scoop and pick up the ball. The main steps of the excavation block calculation are illustrated in figure 5.9.

In the simulation the operator is required to pick up the ball and drop it as close as possible to the centre of a marked area. The block calculates the total time and the distance travelled by the users, as well as the distance from the centre of the marked area of the placed ball.

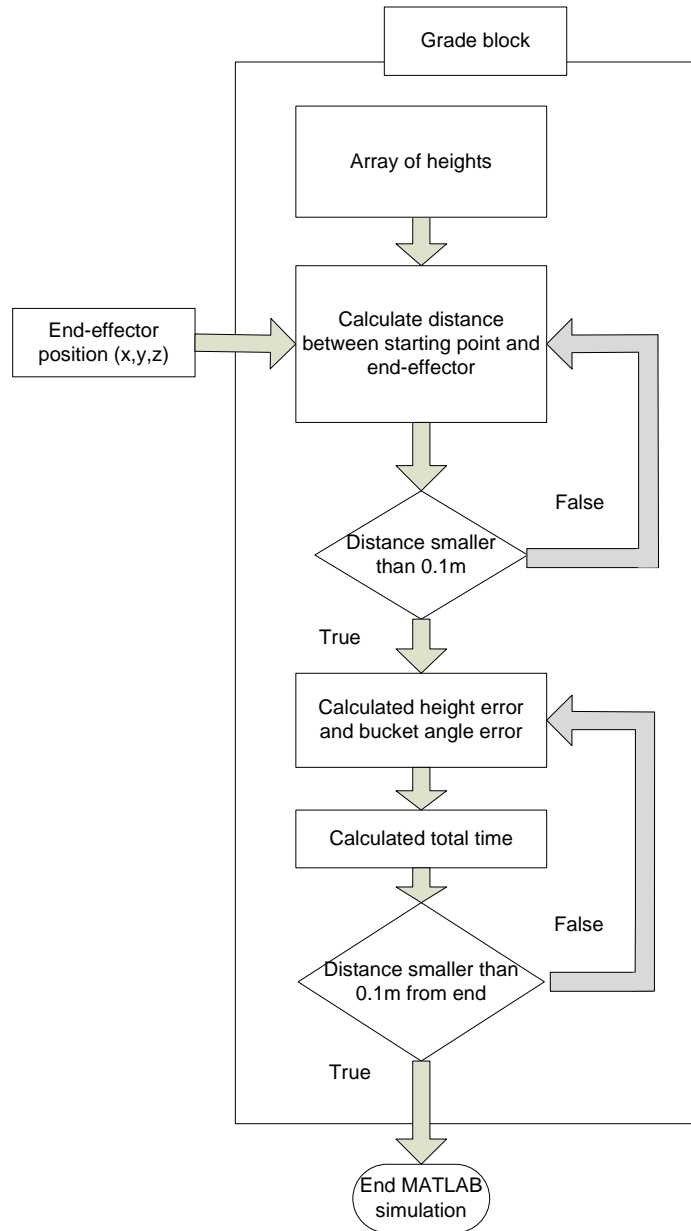


Figure 5.8: Calculation steps of Grade block

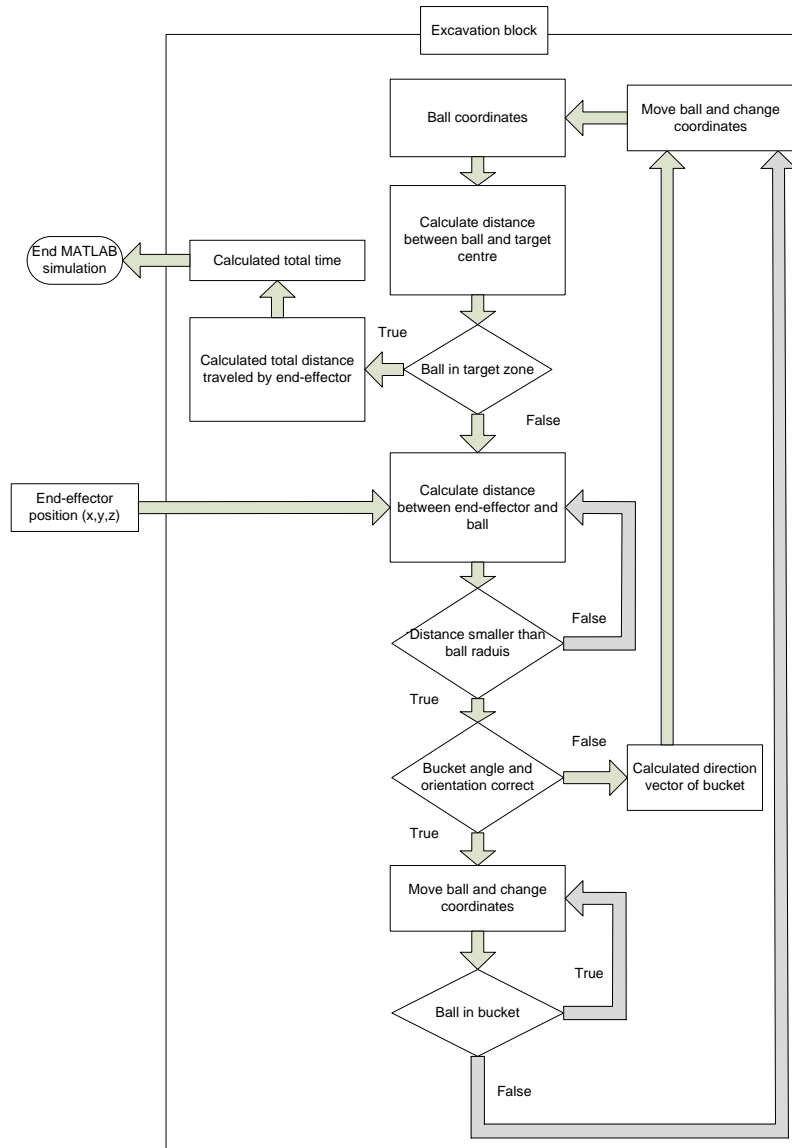


Figure 5.9: Calculation steps of Excavation block

# Chapter 6

## Test procedures and results

In this chapter all aspects of the tests performed by the inexperienced operators will be discussed and illustrated. Four tests were performed by each of the 10 users, and the results of each test are illustrated and discussed in the sub sections. The goal was to test the ergonomic aspect of the two input layouts; and not to assess excavator operator skill as had been done by Bernold [1], but rather to try to compare the ability of the two input layouts to facilitate learning. The testing of the ergonomic aspects can be divided into two sections; the intuitive design (input action related to joint angles) and the control aspect (position and position/rate). The three phases of learning are described by Fitts et al. [43] as 1) cognitive; 2) associative; and 3) autonomous. It has been shown that less cognitive thought is needed as the trainee becomes more adept at a task. During the first phase the trainee will constantly be thinking, observing and copying actions. In the second phase no further instructions are needed, the cues are now directly linked to appropriate actions. In the final stage the user no longer has to think about the movement - the actions are smooth and accompanied by integrated patterns. Introducing tests that require the equivalent of the psychomotor skills of excavation tasks made it possible to compare the first phases of learning as regards the input layout.

The first setup was to perform tests that did not incorporate any feed-

back, force or any numeric indication of the operator's performance (eg the bucket height, measured from the ground, indicated in the corner of the screen). Ten right handed test subjects participated in the test. Each test was repeated three times on each input layout. The task coordinates were varied to prevent the possibility of unreliable results due to repetitive learning. To prevent an order effect, the test method was also varied; completing the tests with either the joysticks or the haptic device first. The data was logged and then compared for each sequence and test. The background, age and hobbies of each user were noted. Testing of the user took about 2 hours with small variations, which depended mainly on the user's performance.

A major problem with the simulator was the user's lack of depth perception due to the 2D projection. A grid at the ground level was added as illustrated in figure 6.1. The test administrator was also present to help the test subject in rotating or changing the operator's view according to the preferred angle, while not allowing unrealistic angles that would give an unfair advantage. None of the test subjects had any prior experience with the haptic device. To normalise the results, each user was given a test run with each test orientation in order to illustrate the given task and to familiarise the user with the method of control (rate or position).

## 6.1 Test 1: Orientation

In this test the user was required to move through designated points in space as illustrated in figure 6.1. A point is indicated by a red sphere and a line directed towards the ground plane, which was drawn to increase depth perception and awareness in 2D space. Once the operator moves the bucket through the point, the point disappears and a new, relocated point is drawn. This prevents path planing and confusion between the multiple points drawn. The two variables that were compared were the distance travelled by the end effector and the time taken to complete the simulation test. Every operator repeated the test with three different target location sets, each target set requiring a specific amount of effort. The

amount of effort required is related to the distance between the points as well as to change in direction. Figure 6.2 illustrates the movement by an operator through the marked points in space, where the default starting point of the end-effector/bucket is indicated by an  $x$ .

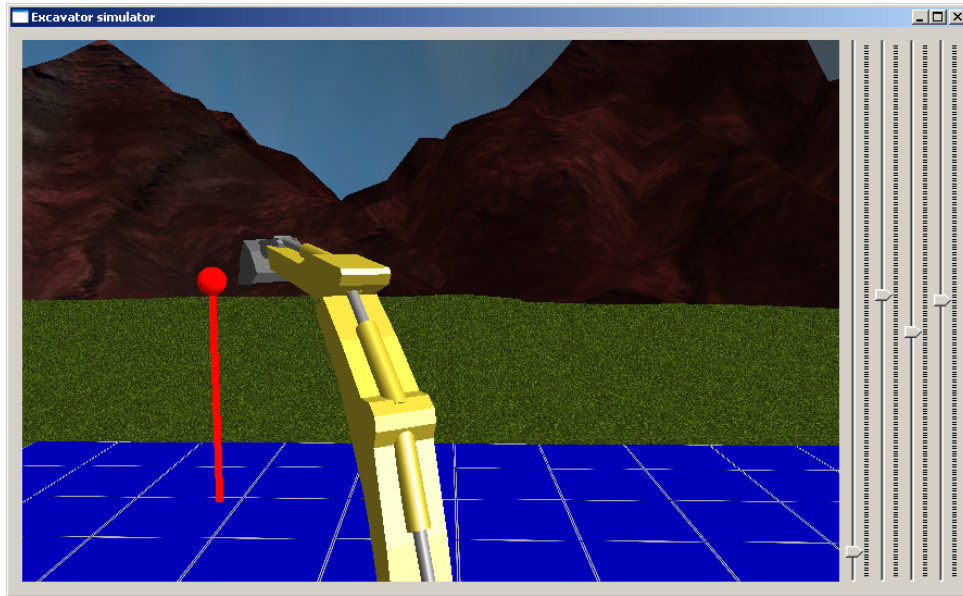


Figure 6.1: Screenshot of test 1 - Orientation

Figure 6.4 compares and illustrates the averages for each user of the orientation test. From figure 6.4 it can be seen that there is an average improvement between the actual controls and haptic device of 27% in the amount of effort required (distance) as well as a 35% improvement in the time taken. The time and distance relationship of all 3 repetitions, for each user, is noted figure 6.3. The colour-coded time and distance relation for each user is drawn and numbered accordingly. The length and gradient of the line represents the overall improvement. It may also be noted, in figure 6.3, that most of the users' haptic performances are closely grouped, indicating that the operation of the haptic device is not heavily dependent on the user's psychomotor skills.

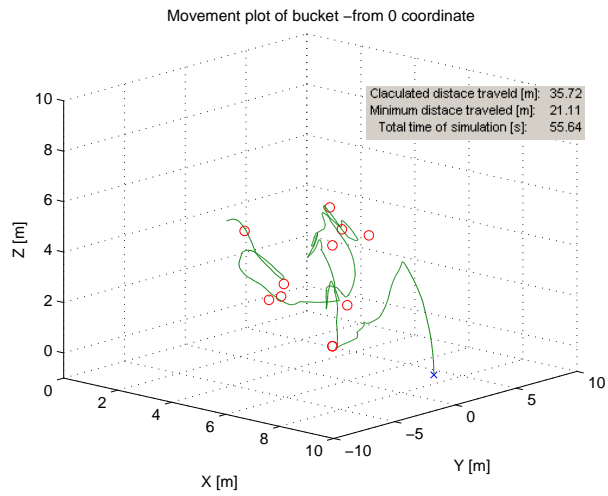


Figure 6.2: Test 1 completed with joystick

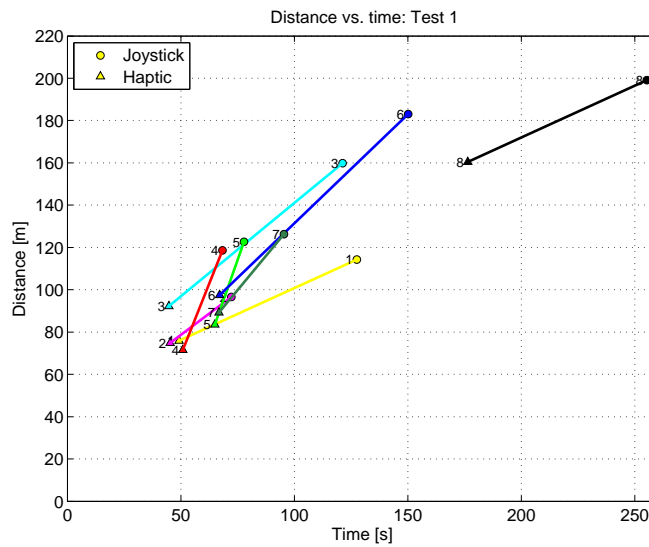


Figure 6.3: Distance vs. time: Test 1 - Orientation

### 6.1.1 Comments on test 1

- When tested using the joysticks, the users did not attempt to remember the excavator link angles relative to the control input, but rather learnt by trial and error; moving the joystick through several positions until the desired command position was found.

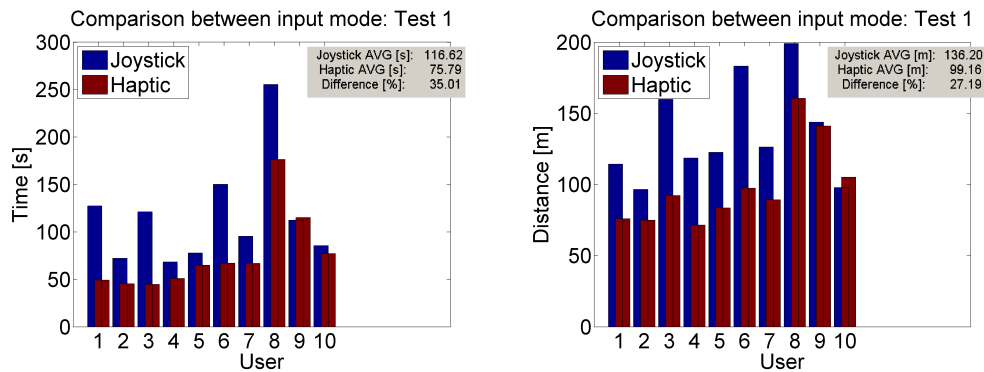


Figure 6.4: User results of test 1 - Orientation

- The most noted positive reply by the users was that "the haptic device was more intuitive and simplified the tests".
- Three main complaints were 1) the sensitivity of the wrist mode and 2) the lack of feedback and 3) the inability to feel the range of the position control.

## 6.2 Test 2: Following desired trajectory

In this test the user is instructed to follow a desired trajectory which is plotted on the screen. The desired trajectory is illustrated by a red line, and the origin is marked with a sphere marker as shown in figure 6.5.

The motor skill that is tested is the user's ability to control each link angle in order to move the bucket according to the illustrated path. In test 2, more skill is required than in test 1. The increase in the level of skill required is due to the "unnatural" path given, which requires small concentrated joystick movements. The test was completed three times by each subject with different given trajectories. The deviation from the given path was measured as the error distance from the line, and was calculated with the trace block set in 5.2.4. Figure 6.6 illustrates the result of an operator's movements through the marked trajectory in space.

Figure 6.8 compares and illustrates the distance averages and stan-

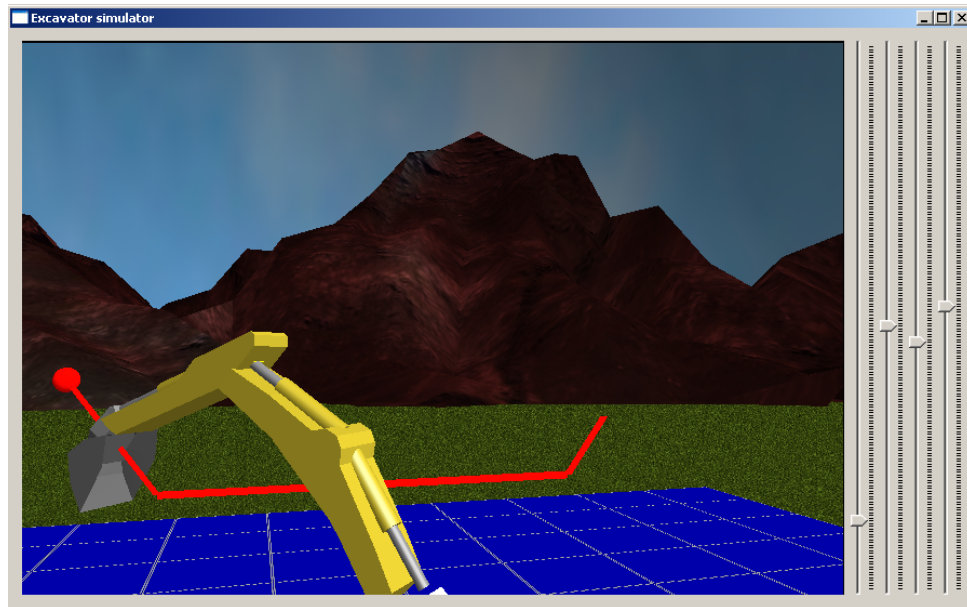


Figure 6.5: Screenshot of test 2 - Following desired trajectory

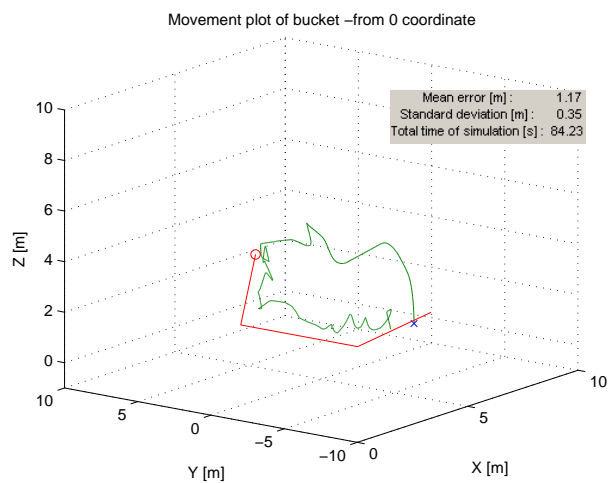


Figure 6.6: Test 2 completed with joystick

dard deviation of each user for the trajectory test. From figure 6.8 it may be seen that there is an average improvement between the actual controls and haptic device of 14% in the error distance from the desired path as well as a 21% improvement in time taken. The standard deviation (SD)

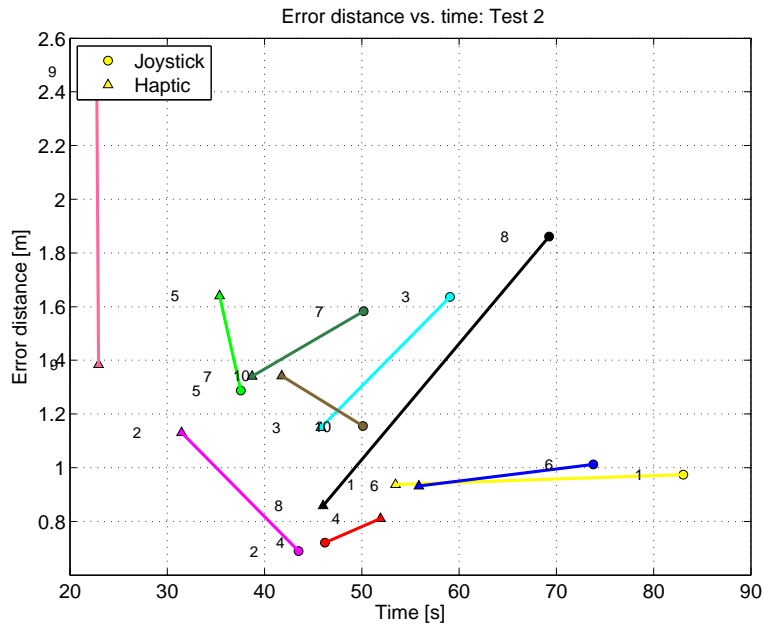


Figure 6.7: Distance vs. time: Test 2 -Following desired trajectory

for the error distance is also illustrated in figure 6.8; the time and distance relationship of all 3 repetitions for each user in figure 6.7. It can also be noted from the results that there is a small improvement in haptic performance. The main reason for loss of proficiency is the wrist swing. Users who performed the test more slowly performed better, in terms of SD as well as distance, because of the sensitivity of the haptic device in the wrist action.

### 6.2.1 Comments on test 2

- The sensitivity problem is caused by the small region of the wrist action that is directly related to the swing. The user struggles to "feel" and differentiates between the different regions of control (position or rate). When a fine position control action is needed, the user accidentally positions the haptic device in rate mode, overshooting the desired point, whereas the original joystick orientation is always automatically positioned.

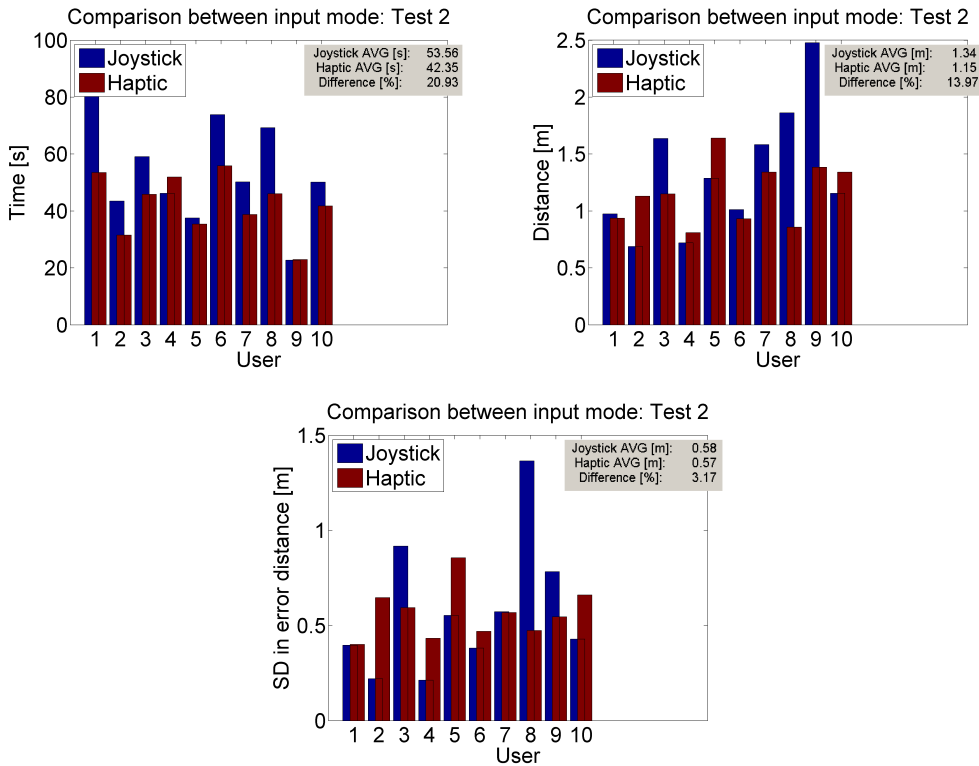


Figure 6.8: User results of test 2 - Following desired trajectory

### 6.3 Test 3: Grading

In the grading test the user was asked to follow a trajectory that resembles that of the grading of a trench. The focus should be to control the height, as well as the angle, of the bucket. The grade block in 5.2.4 was used to calculate the angle and height error. The following describes the joystick actions needed to perform the trenching exercise, as illustrated in 6.9.

1. A starting point and height should be defined - either the bottom of the trench or the surface that needs to be graded.
2. The boom should be extended and the dipper lowered to the specified starting point.

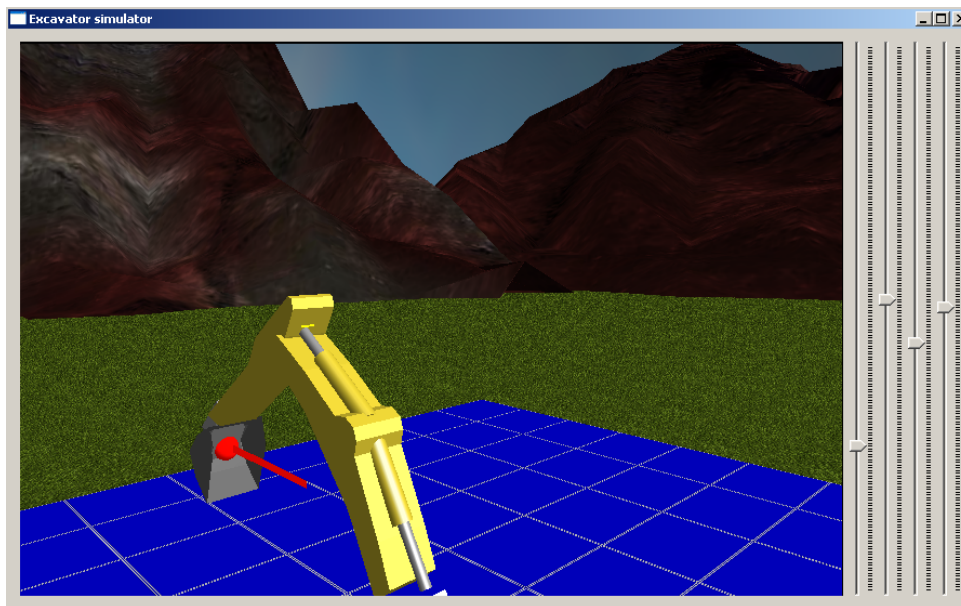


Figure 6.9: Screenshot of test 3 - Grading

3. The bucket should be at the correct angle: ie be horizontal to the ground in order to produce a smoothing action, not digging.
4. The dipper should then be pulled towards the excavator whilst the height is controlled by the boom. It should be noted that as the dipper is brought closer to the excavator, the boom is also raised. The boom should be raised less as the bucket gets closer and is slowly lowered as the dipper passes the vertical midway point.
5. Whilst controlling the height of the bucket with the boom and dipper input, the bucket should be opened. The bottom of the bucket should stay horizontal to the ground to produce a smooth grade or surface.

The grade test is illustrated in figure 6.11, where the user was asked to perform the grading task at 3 different heights. The change in height prevented repetitive learning and, instead, tested the operators ability to perform multiple input tasks.

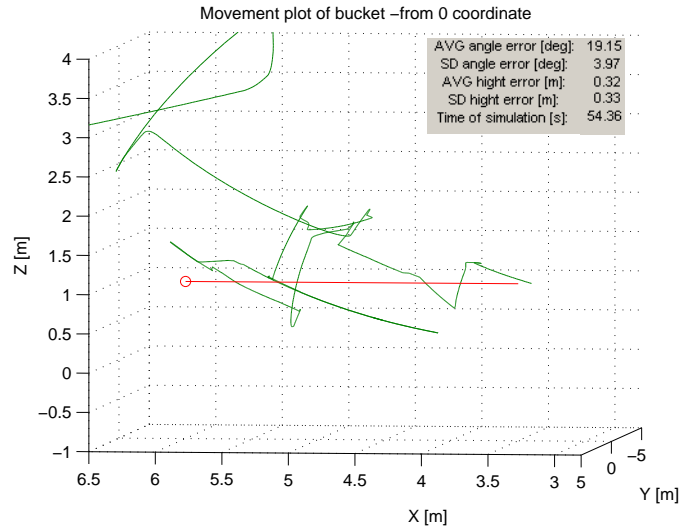


Figure 6.10: Test 3 completed with joystick

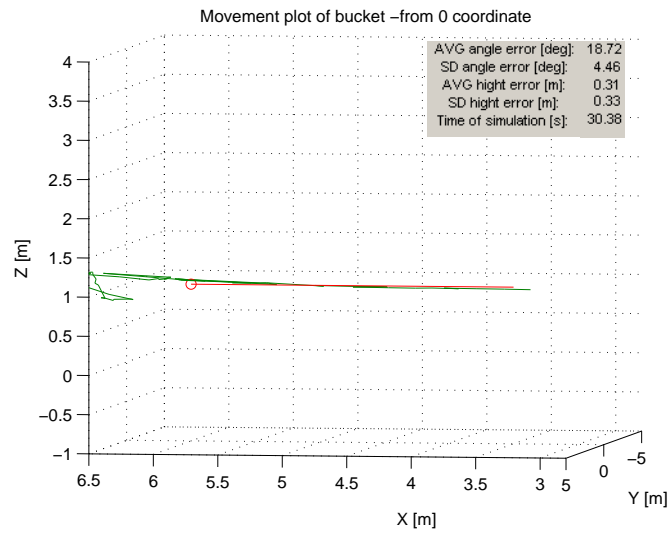


Figure 6.11: Test 3 completed with haptic device

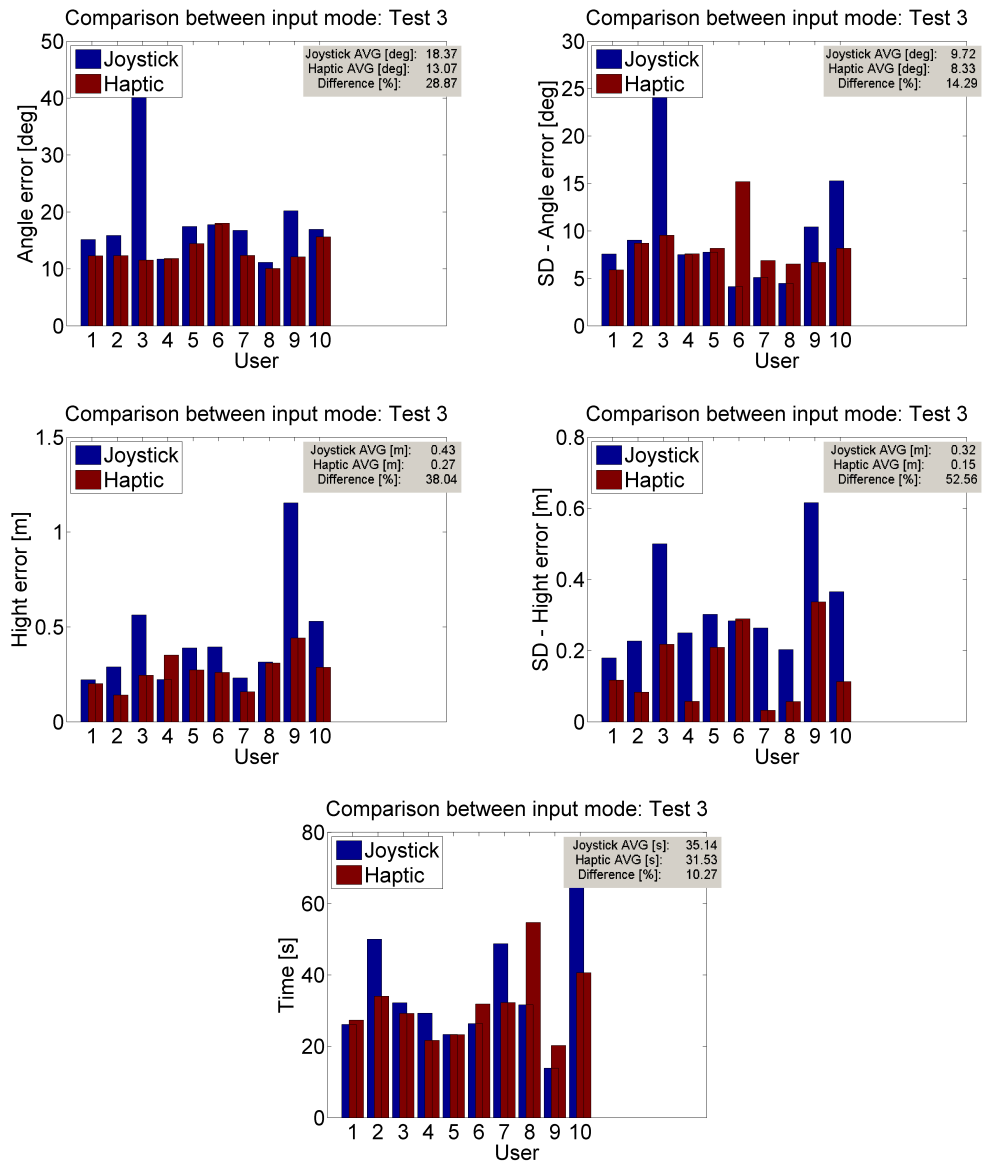


Figure 6.12: User results of test 3 - Grading

Figure 6.12 compares and illustrates the distance averages and standard deviation of each user for the grading test. From figure 6.12 it can be seen that there is an average improvement of 28% in the angle error as well as a 14% improvement in the standard deviation (SD) in angle error. It may be noted that the greatest improvement is in height error (38%) and in SD of height error(52%). The mean height error was calculated by using the statistical tools described in the statistical summary - Appendix A.

### 6.3.1 Comments on test 3

- In this test exercise the haptic device had the major advantage of relating a single input to the end-effector height. The user had only to establish the correct height and starting point and then pull the main lever towards himself, while focusing only on controlling the bucket angle.
- One drawback of the haptic device was the wrist rotation coupling; as the operator pulls the main lever towards himself, he rotates his wrist slightly, inducing a slight swing action.
- A major task the users struggled to cope with, was to control the bucket angle whilst simultaneously controlling the height. Most of the users focused only on the dipper height and not the end effector height. This can clearly be seen in figure 6.12. The same action was also noted in the haptic tests, but the user responded better in these tests after realising the error.

## 6.4 Test 4: Excavation

In the final test the operator is required to pick up a ball and to place or drop the ball at a marked location. The picking up and dropping of the ball resembles the action of an excavation task. The collecting of the ball is illustrated in figure 6.13. The desired drop zone is marked with a red

cross; also seen in figure 6.13. The excavation test is a combination of the first 3 tests, with the operator being required to position the bucket behind the ball, where after the boom and dipper should be pulled in, while closing the bucket.

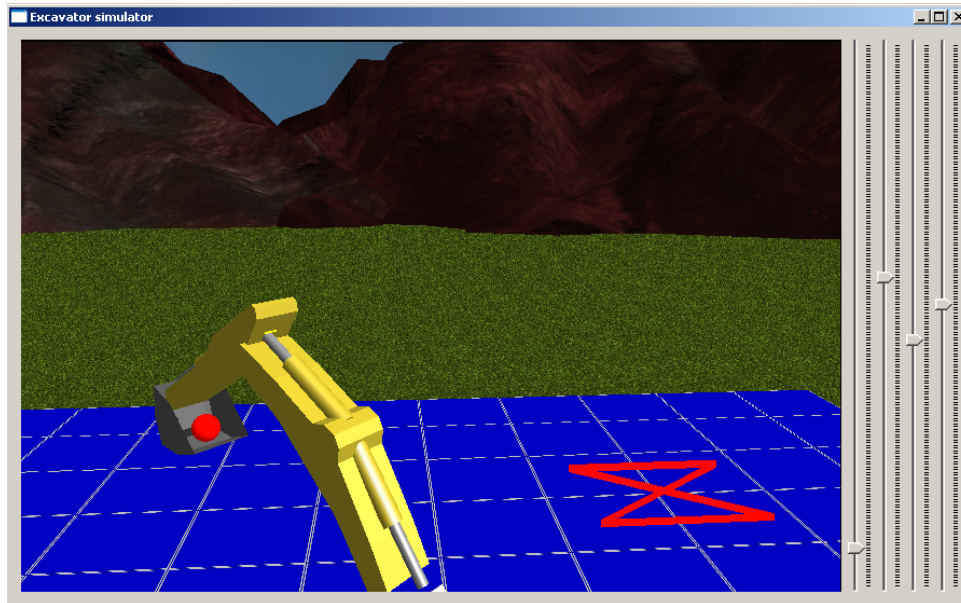


Figure 6.13: Screenshot of test 4 - Excavation

The ball was modelled as a rigid object and it can also be pushed or moved around by the end effector. The variables of interest were the time taken to complete the simulation and the distance travelled by the end effector. Figure 6.16 illustrates and compares the average distances of each user for the excavation test. From figure 6.16 it can be seen that there is an average improvement of 51% in the amount of effort (distance) as well as a 39% improvement in time taken for the test.

#### 6.4.1 Comments on test 4

- A positive comment made by most of the users was that the " bucket control via the trigger was much easier and more intuitive than the original joystick orientation".

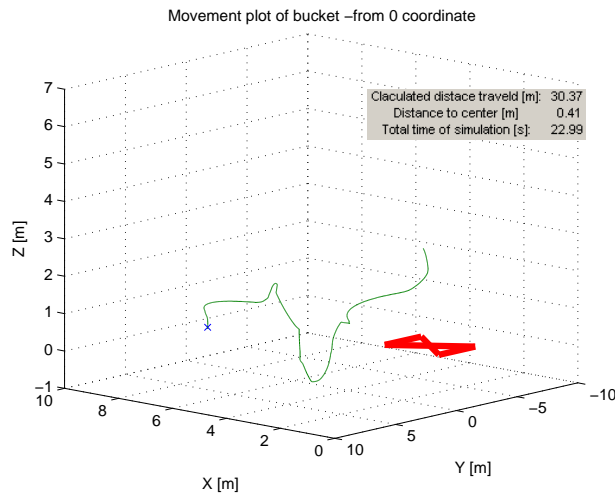


Figure 6.14: Test 4 completed with joystick

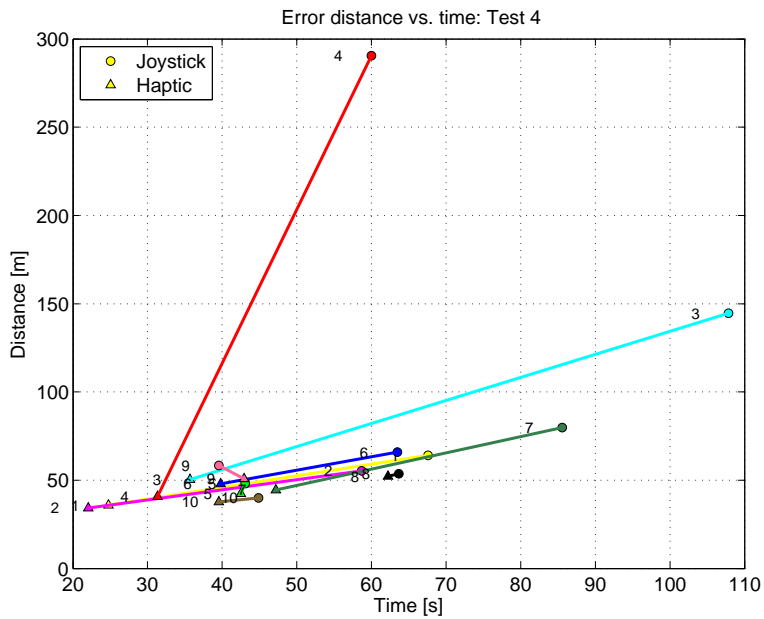


Figure 6.15: Distance vs. time: Test 4 - Excavation

- Only two users struggled to scoop the ball the first time, either accidentally moving the ball or dropping it whilst moving it towards the marked zone.

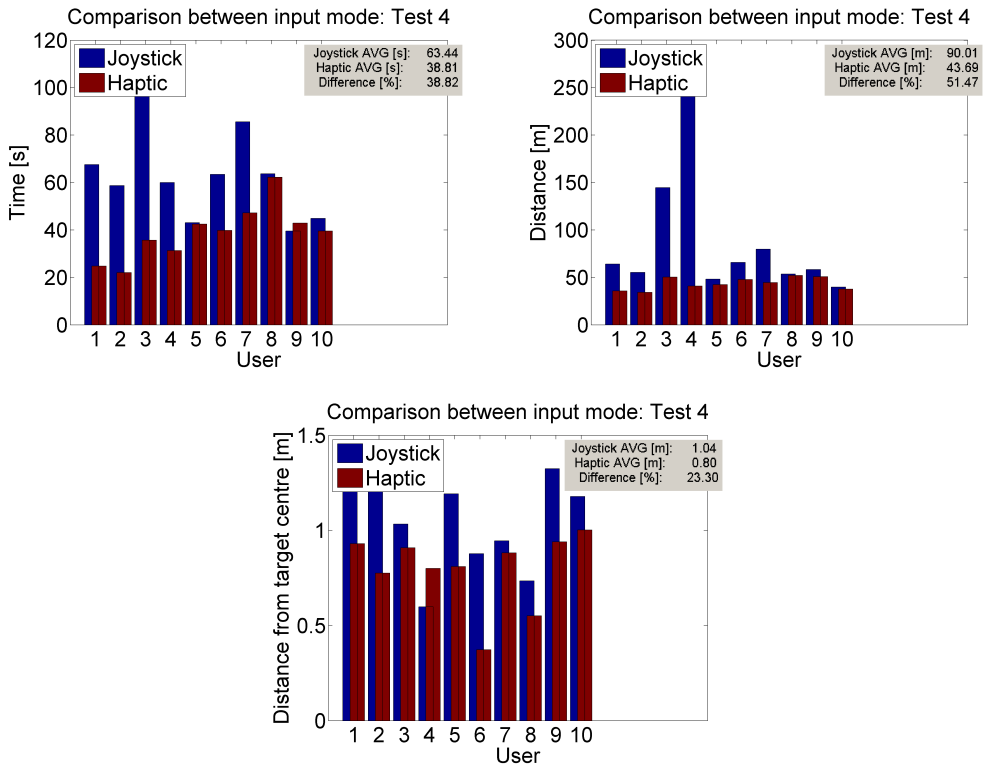


Figure 6.16: User results of test 4 - Excavation

## 6.5 Summary and discussion

A summary of all four tests are listed in table 6.1. From the tests and results it can be noted that the three main human factors tested where effort, precision and time. The effort of performing the task was measured as the distance which the end-effector travelled for each task, and was measured for test 1 and 4. Precision, measured in test 2 and 3, was the operators ability to move the end-effector in a specified path or keeping it at a correct angle and height. Time depicts the amount of time that the operator needed to complete each test and was measured in all four tests. The summary for the three main operator factors tested are listed in table 6.2.

The results strongly support the hypothesis that the coordinated haptic control simplifies the operational tasks required for operating an exca-

Test nr:	Effort(distance)	Angle -error	Height-error	Track-error	Time
1	27%	-	-	-	35%
2	-	-	-	14%	21%
3	-	28%	38%	-	10%
4	51%	-	-	-	39%

Table 6.1: Summary of the average improvement for the four tests

Test nr:	Effort(distance)	Precision	Time
1	27%	-	35%
2	-	14%	21%
3	-	33%	10%
4	51%	-	39%
AVG	39%	24%	26%

Table 6.2: Summary of the three main improved areas

vator. The average results for the haptic device outperformed joysticks in all the tests and the performance could further be improved if the haptic device were calibrated according to each user's liking. The haptic device requires fewer psychomotor skills, due to the user requiring only one hand for operation. The haptic device requires mechanical improvement of the linear actuator in order to produce a smoother action, which would improve the ease of use. It was noted that some of the users struggled to control the haptic device; this was mainly due to the sensitivity of the load cell controlling the linear actuator.

Most of the test subjects were students, some of the students had a great deal of experience of computer games, which could be clearly noted in the test. The students who had been exposed to computer games (users 1,4,5) outperformed the other users on the joysticks, due to their greater psychomotor skills. A test subject (user 8) from the local construction industry was also tested. The test subject had prior experience with ground moving equipment (as a soil-truck driver) but no practical experience of operating an excavator or backhoe, and was a typical example of an operator that might need to be trained.

The implementation of the haptic device in hydraulic machinery can

have several advantages that could lead to higher production output and an increase in safety. From these results and those in Wallerstainer et al. [7] it can be assumed that an experienced operator will perform with the same proficiency as usual using the haptic device, within a relatively short amount of time. This is due to the fact that the haptic device design requires fewer psychomotor skills, thus creating a faster learning curve.

# Chapter 7

## Summary and recommendations

### 7.1 Summary

This thesis has presented the design and practical test results obtained for the haptic device which was constructed. A concept model of the haptic device was developed after the work space and degrees of freedom of an excavator had been studied. The haptic device was constructed at a relatively low cost compared to commercially available haptic devices.

The haptic device constructed consists of several actuators that could provide feedback when needed. Further studies and experiments with force feedback implemented can improve the current obtained user performance and reduce training time [1].

Kinematic equations used in the control algorithms were derived and programmed via MATLAB. A virtual excavator simulator was developed, where the human factors, related to the input orientation were tested. The virtual excavator which was developed consisted of a graphical user interface and test blocks in MATLAB. The graphical interface was developed in QT and only functioned as a display mechanism for 3D rendering. The coordinate and joint angles for the excavator links were given via the MATLAB server, where the test blocks then calculated the required variables (time, distance and error).

The results indicated that, on average, all the users performed better

with the haptic device. The improvement was measured in terms of effort, precision and time taken to complete the test and is listed in 6.5. The results strongly support the hypothesis that the coordinated haptic control simplifies the operational tasks required for operating an excavator.

The results obtained can act as a reference point for further haptic development, as there is very little research available on the haptic design based on human factor testing for the setup of excavator control.

## 7.2 Recommendations

The scope of the project is an extremely large one, where every division - hydraulic control, haptic design and haptic control - is a research field on its own. The following are the main recommendations on how the current system can be improved.

### 7.2.1 General

Developing a haptic device that produces smooth actions and feels correct for the operator in terms of force feedback and robustness can be very time consuming and can only be achieved after a great deal of testing and many calibrations. The haptic device which was developed is only a prototype, for which the control and orientation was tested. There is room for several improvements to the calibration of the haptic device in order to produce a smooth output and get the correct feel. The next and final step would be practical implementation of the haptic device in an excavator. This would require extensive hydraulic control system modelling and electronic integration.

### 7.2.2 Mechanical

- The linear actuator design suffers from mechanical friction between the threaded rod and the gears. The simplest solution to this problem would be to use a rod with a smaller thread pitch, creating a smoother action and resulting in higher resolution.

- The wrist action sensor requires a high resolution, because of the small workspace available. A way of resolving the problem would be to implement only rate control on the wrist action, as the swing actuator is used only for large control movements.
- The wrist and trigger action could be further improved if feedback were added to each. This would allow the user to feel the different control regions as well as giving an increased awareness of the operating surroundings.
- The POTs used are sufficient, but higher resolution sensors would enable finer control - especially for the wrist action. This applies in general, although most of the components used are simple and cheap, these components are not suitable if greater precision is required.

### 7.2.3 Control

- Several additional control algorithms are available, and an interesting study could be done on these control algorithms as implemented on the haptic device.
- Feedback is one of the essential components of the haptic device, and should be modelled. There are several simple models available [11],[19] that could be used and which can be tested on the current haptic device setup.

### 7.2.4 Simulator

With the current simulator the main focus was on the control of the end effector and the orientation. For greater realism the response of the bucket to the environment could be modelled, providing the operator with additional feedback on the training and better evaluation.

- The first significant improvement on the current simulator would be graphic illustration of the soil and bucket interaction, so that the

operator would have the ability to dig a trench with the soil reacting realistically.

- The bucket-soil interaction could be modelled, as could the excavator dynamics during the soil interaction.
- An obstacle detection and avoidance test could also be implemented, where the operator would dig a trench around hidden objects (eg electrical pipelines), and where the feedback provided by the haptic device would act as a guide to detecting the hidden objects.

# Appendices

# Appendix A

## Statistical summary

Here is a summary of the statistical tools used in the human factor testing of chapter, 6. If the random variable  $X$  takes on  $n$  values where the data set is given by:

$$X = \{x_1, x_2, \dots, x_n\} \quad (\text{A.0.1})$$

$$\bar{x} = \frac{\sum_{i=1}^n x_i}{n} \quad (\text{A.0.2})$$

$$\sigma = \sqrt{\frac{1}{n-1} \sum_{i=1}^n (x_i - \bar{x})^2} \quad (\text{A.0.3})$$

where  $\bar{x}$  is the sample mean and  $\sigma$  is the square root of the sample variance (standard deviation) assuming normal distribution.

# **Appendix B**

## **Design dimensions**

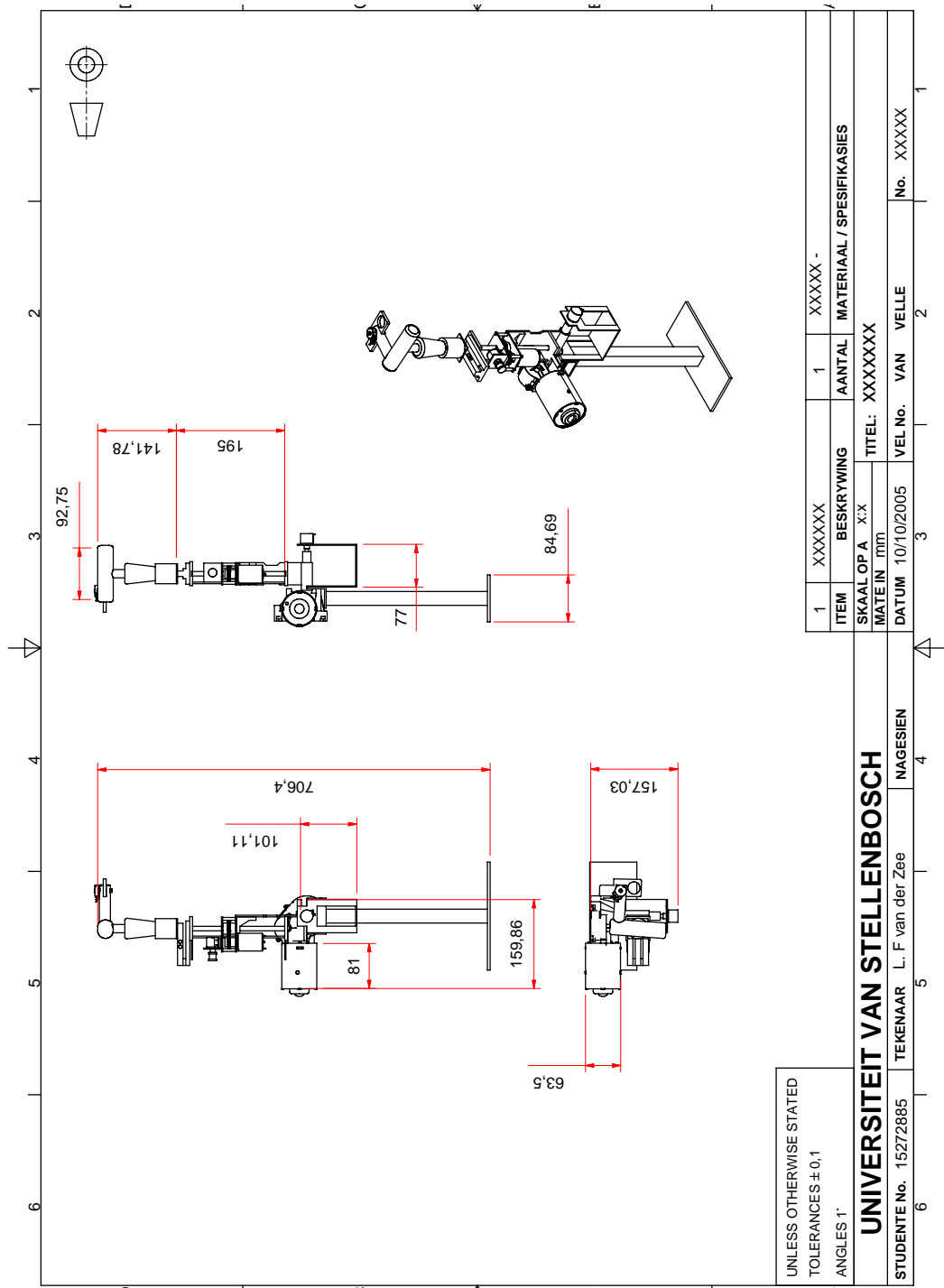


Figure B.1: General dimensions of haptic device

# Appendix C

## Hardware details

H-bridge	
Supply voltage	12V
Supply current	2mA
Input signals:	0-5V
ALI	
BLI	
AHI	
BHI	
Load/motor voltage	10V
Load/motor current	15A
General dimension	110x85mm

Table C.1: H-bridge PC board details

dsPIC -motor controller	
Supply voltage	5V
Supply current	200mA
Input signals:	0-5V
Strain gage	
Load cell	
Wrist POT	
Trigger POT	
Linear POT	
Rotation POT	
General dimension	130x85mm

Table C.2: dsPIC PC board details

Opto-coupler	
Supply voltage	5V
Supply current	5mA
Input signals:	0-5V
ALI	
BLI	
AHI	
BHI	
General dimension	55x80mm

Table C.3: Opto-coupler PC-board details

Strain gauge amplifier	
Supply voltage	5V $\pm$ 12V
Supply current	5mA
Input signals:	0-5V
Strain gauge	
Rotation POT	
Wrist POT	
General dimension	50x80mm

Table C.4: Stain gauge PC-board details

Load cell amplifier	
Supply voltage	5V, $\pm 12V$
Supply current	5mA
Input signals:	
Load cell	
Trigger POT	
Linear POT	
General dimension	50x80mm

Table C.5: Load cell PC-board details

Input		Output			
ALI,BLI	AHI,BHI	U/V	DIS	ALO,BLO	AHO,BHO
X	X	X	1	0	0
1	X	0	0	1	0
0	1	0	0	0	1
0	0	0	0	0	0
X	X	1	X	0	0

Table C.6: Truth table for the HIP4081; X signifies that input can be either a 1 or 0

# Bibliography

- [1] L. E. Bernold, "Quantitative assessment of backhoe operator skill", *Journal of construction engineering and management*, vol. 133, Nov. 2007.
- [2] Paul Coughlin., "How to operate a backhoe", Sept. 2006, e book from <http://www.backhoetips.com>.
- [3] O. Luengo and A. Barrientos, "Telemanipulation and supervisory control of a backhoe excavator", in *SPIE Conference on Telemanipulator and Telepresence Technologies*, 1998.
- [4] S. Tafazoli, P. D. Lawrence, and F. Salcucean, "Identification of inertial and friction parameters of excavator arm", *IEEE Transactions on robotics and automation*, vol. 15, no. 5, Oct. 1999.
- [5] S. Tafazoli, P. D. Lawrence, S. E. Salcucean, D. Chan, S. Bachmman, and S. W. Silva, "Parameter estimation and friction analysis for a mini excavator", *IEEE int Conf. on Robotics and Automation*, Apr. 1996.
- [6] A. Stentz, J. Bares, S. Singh, and P. Rowe, "A robotic excavator for autonomous truck loading", *Proceedings of International Conference of Intelligent Robots and System*, Oct. 1998.
- [7] U. Wallerstainer, P. Lawrence, and B. Sauder, "A human factors evaluation of two different machine control systems for log loaders", *Ergonomics*, vol. 26, pp. 927–934, Aug. 1993.

- [8] M. E. Kontz, J. Beckwith, and W. J. Book, "Evaluation of a tele-operated haptic forklift", *Proceedings of International Conference of Advanced Intelligent Mechatronics*, pp. 295–300, Jul. 2005, Monterey, CA.
- [9] J. Fritz and K. Barner, "Design of a haptic data visualization system for people with visual impairments", *IEEE Transactions on Rehabilitation Engineering*, vol. 7, pp. 372–384, Sept. 1999.
- [10] M. A. Peshkin, J. E. Colgate, W. Wannasuphprasit, C. A. Moore, R. B. Gillespie, and P. Akella, "Cobot architecture", *IEEE Transactions on Robotics and Automation*, vol. 17, Aug. 2001.
- [11] S. E. Salcudean, K. Hashtrudi-Zaad, S. Tafazoli, S. P. DiMaio, and C. Reboulet, "Bilateral matched-impedance teleoperation with application to excavator control", *IEEE Control Systems*, pp. 29–37, Dec. 1999.
- [12] S. Singh, "State of the art in automation of earthmoving," *Journal of Aerospace Engineering*, pp. 179–188, Oct. 1997.
- [13] Alleyne A. and Liu R., "A simplified approach to force control for electrohydraulic systems", *Control Engineering Practice*, pp. 1347–1356, 2000.
- [14] Q. H. Nguyen, Q. P. HA, D. C. Rye, and H. F. Durrant Whyte, "Impedance control of a hydraulically actuated robotic excavator", *Automation and construction*, pp. 421–435, 2000.
- [15] Q. H. Nguyen, Q. P. Ha, D. C. Rye, and H. F. Durrant Whyte, "Force /position tracking for electrohydraulic systems of a robotic excavator", *39<sup>th</sup> IEEE Conference on decision and control*, pp. 5224–5229, 2000.
- [16] P. D. Lawrence, S. E. Salcudean, N. Sepeshri, D. Chan, S. Bachmann, N. Parker, M. Zhu, and R. Frenette, "Coordinated and force feed-

- back control of hydraulic excavators", *4<sup>th</sup> International Symposium on Control and Information*, pp. 181–194, June 1995.
- [17] J. G. Frankel, "Development of a haptic backhoe testbed", Master's thesis, Georgia Institute of Technology, 2004.
- [18] M. Kontz, *Haptic control of hydraulic machinery using proportional valves*, PhD thesis, Georgia Institute of Technology, 2007.
- [19] J. Yan and S. E. Salcudean, "Teleoperation controller design using  $h_{\infty}$  optimisation with application to motion-scaling", *IEEE Transactions on Control Systems Technology*, pp. 244–258, May 1996.
- [20] J. J. Craig, *Introduction to Robotics*, Addison-Wesley Pub. Co., 1989.
- [21] L. Sciavicco and B. Siciliano, *Modeling and Control of Robot Manipulators*, London: Springer-Verlag, 2<sup>nd</sup> edition, 2001.
- [22] A. J. Koivo, M. Thoma, E. Kocaoglan, and J. Andrade-Cetto, "Modelling and control of excavator dynamics during digging operation", *Journal of Aerospace Engineering*, pp. 10–18, Jan. 1996.
- [23] L. W. Tsai, *Robot Analysis*, John Wiley and Sons, 1999.
- [24] E. Papadopoulos, B. Mu, and R. Frenette, "On modeling, identification, and control of a heavy-duty electrohydraulic harvester manipulator", *IEEE/ASME Transactions on Mechatronics*, vol. 8, June 2003.
- [25] S. P. DiMaio and S. E. Salcudean, "A virtual environment for the simulation and programming of excavation trajectories", *Presence*, vol. 10, Oct. 2001.
- [26] W. E. Allen P. D. Anderson, W. J. Bradbury, J. M. Hadank, and R. B. League, "Coordinated control for a work implement", United States Patent (5,160,239), Nov. 1992.

- [27] W. E. Allen P. D. Anderson, W. J. Bradbury, J. M. Hadank, and R. B. League, "Coordinated control for a work implement", United States Patent (5,424,623), Jun. 1995.
- [28] E. G. Brandt and B. D. Rickwood, "Apparatus and method for providing coordinated control of a work implement", United States Patent (6,374,153), Apr. 2002.
- [29] C. T. Brickner, E. Bright, C. L. Padgett, and W. C. Swick, "Method of modulating a boom assembly to perform in a linear manner", United States Patent (7,040,044), May 2006.
- [30] A. D. Berger, P. J. D. D. C. Chan, and J. M. Grupka, "Electronic control for a two-axis work implement", United States Patent (6,233,511), May 2001.
- [31] A. D. Berger and K. B. Patel, "Electronic coordinated control for two-axis work implement", United States Patent (6,115,660), Sep. 2000.
- [32] S. S. Hendron, J. P. Clark, and B. D. Sulzer, "Automatic loader bucket orientation control", United States Patent (6,763,619), Jul. 2004.
- [33] S. S. Hendron and J. P. Clark, "Automatic loader bucket orientation control", United States Patent (6,609,315), Aug. 2003.
- [34] T. Hirata, E. Yamagata, H. Watanabe, M. Haga, K. Fujishima, and H. Adachi, "Region limiting excavation control system for construction machine", United States Patent (5,835,874), Nov. 1998.
- [35] H. Watanabe, K. Fujishima, and M. Haga, "Slope excavation controller of hydraulic shovel, target slope setting device and slope excavation forming method", United States Patent (6,076,029), Jun. 2000.
- [36] H. Watanabe, T. Hirata, M. Haga, and K. Fujishima, "Excavation area setting system for area limiting excavation control in construction machines", United States Patent (5,960,378), Sep. 1999.

- [37] B.W. Kraft, "Force feedback control for backhoe", United States Patent (5,019,761), May. 1991.
- [38] R.W. Daniel and P.R McAree, "Fundamental limits of the performance for force reflecting teleoperation", *International journal of robotics research*, vol. 17, no. 8, pp. 811–830, Aug. 1998.
- [39] H.Z. Tan, B. Eberman, M. A. Srinivasan, and B. Cheng, "Human factors for the design of force-reflecting haptic interfaces", *Proc of ASME WAN*, vol. 55-1, pp. 353–360, 1994, ASME NY.
- [40] S. Lee, P. H. Chang, and Y. Kwon, "An experimental study on cartesian tracking control of automated excavator system using tdc-based robust control design", *Proceedings of the American Control Conference*, Jun 1999.
- [41] Joseph E. Shigley, Charles R. Mischke, and Richard G Budynas, *Mechanical Engineering Design*, McGraw-Hill companies Inc, 7<sup>th</sup> edition, 2004.
- [42] R. Busch, "Modelling and simulation of an autonomous underwater vehicle", Master's thesis, University of Stellenbosch, Department of Electrical Engineering, Private Bag X1 ,7602 Matieland, South Africa, Oct. 2008.
- [43] P. M. Fitts and M. I. Posner, *Human performance*, Brooks/Cole, 1967, Belmont Calif.